Towards Skill Transfer via Learning-Based Guidance in Human-Robot Interaction

Seyed Ehsan Zahedi

A thesis

In the Department

of

Mechanical, Industrial and Aerospace Engineering

Presented in Partial Fulfillment of the Requirements

For the Degree of

Doctor of Philosophy (Mechanical Engineering) at

Concordia University

Montreal, Quebec, Canada

November 2017

Concordia University
School of Graduate Studies

This is to certify that the thesis prepared

By: **Mr. Seyed Ehsan Zahedi**

Entitled: **Towards Skill Transfer via Learning-Based Guidance in Human-Robot Interaction**

and submitted in partial fulfillment of the requirements for the degree of

Doctor of Philosophy (Mechanical Engineering)

complies with the regulations of this University and meets the accepted standards with respect to originality and quality.

Signed by the final examining commitee:

_____ Chair
Dr. Thomas Fevens

_____ External Examiner
Dr. Mahdi Tavakoli

_____ External to Program
Dr. Yousef R. Shayan

_____ Examiner
Dr. Wen-Fang Xie

_____ Examiner
Dr. Narayanswamy R. Sivakumar

_____Thesis Supervisors
Dr. Javad Dargahi

_____
Dr. Mehrdad Zadeh

Approved by   _____
Dr. Ali Dolatabadi, Graduate Program Director

December 19, 2017
_____
Date of Defence

_____
Dr. Amir Asif, Dean
Faculty of Engineering and Computer Science

Abstract

Towards Skill Transfer via Learning-Based Guidance in Human-Robot
Interaction

Seyed Ehsan Zahedi, Ph.D.
Concordia University, 2017

This thesis presents learning-based guidance (LbG) approaches that aim to transfer
skills from human to robot. The approaches capture the temporal and spatial informa-
tion of human motions and teach robot to assist human in human-robot collaborative
tasks. In such physical human-robot interaction (pHRI) environments, learning from
demonstrations (LfD) enables this transferring skill. Demonstrations can be provided
through kinesthetic teaching and/or teleoperation. In kinesthetic teaching, humans
directly guide robot's body to perform a task while in teleoperation, demonstrations
can be done through motion/vision-based systems or haptic devices. In this work,
the LbG approaches are developed through kinesthetic teaching and teleoperation in
both virtual and physical environments.

First, this thesis compares and analyzes the capability of two types of statisti-
cal models, generative and discriminative, to generate haptic guidance (HG) forces as
well as segment and recognize gestures for pHRI that can be used in virtual minimally
invasive surgery (MIS) training. In this learning-based approach, the knowledge and
experience of experts are modeled to improve the unpredictable motions of novice
trainees. Two statistical models, hidden Markov model (HMM) and hidden Condi-
tional Random Fields (HCRF), are used to learn gestures from demonstrations in a
virtual MIS related task. The models are developed to automatically recognize and
segment gestures as well as generate guidance forces. In practice phase, the guidance
forces are adaptively calculated in real time regarding gesture similarities among user
motion and the gesture models. Both statistical models can successfully capture the
gestures of the user and provide adaptive HG, however, results show the superiority
of HCRF, as a discriminative method, compared to HMM, as a generative method,
in terms of user performance.

In addition, LbG approaches are developed for kinesthetic HRI simulations that aim to transfer the skills of expert surgeons to resident trainees. The discriminative nature of HCRF is incorporated into the approach to produce LbG forces and discriminate the skill levels of users. To experimentally evaluate this kinesthetic-based approach, a femur bone drilling simulation is developed in which residents are provided haptic feedback based on real computed tomography (CT) data that enable them to feel the variable stiffness of bone layers. Orthepaedic surgeons require to adjust drilling force since bone layers have different stiffness. In the learning phase, using the simulation, an expert HCRF model is trained from expert surgeons demonstration to learn the stiffness variations of different bone layers. A novice HCRF model is also developed from the demonstration of novice residents to discriminate the skill levels of a new trainee. During the practice phase, the learning-based approach, which encoded the stiffness variations, guides the trainees to perform training tasks similar to experts motions.

Finally, in contrast to other parts of the thesis, an LbG approach is developed through teleoperation in physical environment. The approach assists operators to navigate a teleoperated robot through a haptic steering wheel and a haptic gas pedal. A set of expert operator demonstrations are used to develop maneuvering skill model. The temporal and spatial variation of demonstrations are learned using HMM as the skill model. A modified Gaussian Mixture regression (GMR) in combination with the HMM is also developed to robustly produce the motion during reproduction. The GMR calculates outcome motions from a joint probability density function of data rather than directly model the regression function. In addition, the distance between the robot and obstacles is incorporated into the impedance control to generate guidance forces that also assist operators with avoiding obstacle collisions. Using different forms of variable impedance control, guidance forces are computed in real time with respect to the similarities between the maneuver of users and the skill model. This encourages users to navigate a robot similar to the expert operators. The results show that user performance is improved in terms of number of collisions, task completion time, and average closeness to obstacles.

Acknowledgments

One of the joys of completion is to look over the journey past and remember all the people who have supported and encouraged me along this long but fulfilling journey. Towards working for my PhD, I have had the opportunity to be involved in research work at three universities, including *Concordia University*, *Johns Hopkins University*, and *Kettering University*. I would like to thank everyone who has helped me to accomplish this journey.

I would like to greatly and heartfully thank my co-supervisors, Professors Javad Dargahi and Mehrdad Zadeh, for their nonstop supports, suggestions and direction. This PhD program would not have been possible without their guidance, insightful comments, untiring efforts, encouragement, and patience throughout the development of this program. I would also like to thank members of my defense committee, Professor Yousef R. Shayan, Professor Narayanswamy Sivakumar, and Professor Dr. Wen-Fang Xie, who have helped me throughout my PhD program.

Warm and kind thanks go to all my friends and lab-mates: Alireza Hassanbeiglou, Hadi Rahmat-Khah, Siamak Arbatani, Mostapha Marzban, Amir Hooshiar, and Masoud Razban. Thank you for the joyful memories that I will remember throughout my life.

My sincerest and heartfelt gratitude goes to my parents Narges and AliAkbar who have been always supporting me with their invaluable love as well as my sister Elaheh and my brother Mehdi for encouraging me.

I would like to thank Concordia University and whole staff for preparing such an environment and opportunity for me to carry on my studies to the doctoral level.

Contents

List of Figures

List of Tables

List of Symbols

Symbol	Meaning
j	Instantaneous Jerk (cm/s^3)
AAE	Average Angular Error ($°$)
N	Number of Time Steps
α	Angular Error between the Tangent Vector of User Motion and the Direction of Desired Gesture
x	Position of the End-Effector
$\dot{x}$	Velocity of the End-Effector
$\ddot{x}$	Acceleration of the End-Effector
f_h	Human Applied Force
f_{hg}	Haptic Guidance Force
K_V	Variable Stiffness Gain
λ	HMM Model
P	Probability
π	Prior Probabilities
O	Observation Sequence
S_K	HMM States
$\mathcal{N}$	Gaussian Density
μ	Mean of an HMM State
Σ	Covariance of an HMM State
y	Class Label
Y	Set of Class Labels
θ	Model Parameters
σ^2	Variance of a Gaussian Prior
x	End-effector Position
K_{LbG}	Learning-Based Stiffness Gain
μ	Attenuation Coefficient
θ_s	Angle of Steering Wheel
θ_p	Angle of Gas Pedal
d	Distance to Obstacles
ϕ	Angle to Obstacles
f_{s-h}	Human Input Forces on Steering
f_{p-h}	Human Input Forces on Pedal
f_{s-LbG}	Human Input Forces to Pedal
B_{LbG}	Learning-Based Damping Gain
T_p	Torque Acting on Pedal
T_s	Torque at Steering
ω_r	Angular Velocities of the Right Wheel of Teleoperator
ω_l	Angular Velocities of the Left Wheel of Teleoperator

List of Abbreviations

Abbreviation	Definition
ANOVA	Analysis of Variance
CRF	Conditional Random Fields
D-LbG	Deep Learning-based Guidance
EM	Expectation Maximization
FLS	Fundamental of Laparoscopic Surgery
FOV	Field of View
GMR	Gaussian Mixture Regression
GS	Gesture Similarity
HCRF	Hidden Conditional Random Fields
HG	Haptic Guidance
HMM	Hidden Markov Model
HRI	HumanRobot Interaction
ICR	Instantaneous Center of Rotation
LbD	Learning by Demonstration
L-BFGS	Limited-Memory Broyden-Fletcher-Goldfarb-Shanno (BFGS) Algorithm
LbG	Learning-based Guidance
LfD	Learning from Demonstration
MG-VIC	Multiple-Gain Variable Impedance Control
MIS	Minimally Invasive Surgery
ML	Maximum Likelihood
MS	Motion Similarity or Maneuver Similarity
NG	No Guidance
PbD	Programming by Demonstration
pHRI	physical Human-Robot Interaction
RMSE	Root-Mean-Square Error
SE	Standard Error
SG-VIC	Single-Gain Variable Impedance Control
TC	Computed Tomography
VR	Virtual Reality
VE	Virtual Environment

Chapter 1

Introduction

Human-robot interaction (HRI) is a field of study that aims to design, implement, and assess robotic systems for interacting with humans [2]. An area of interest in this field is to develop methods for transferring knowledge or skill from human to robot. The skilled robots can be used to teach/help other humans to execute dynamic tasks. In other words, this field may promote the transferring of skills from humans (experts) to humans (novices).

1.1 Learning from Demonstration (LfD)

Learning from demonstration (LfD) enable humans, particularly non-robotics-experts, to use demonstration examples for programming robot skills [3]. Traditional robot control approaches usually require the dynamics model of robots to derive mathematical control policies. Developing such models needs considerable expertise. In addition,

linearizing the models decrease the accuracy and performance of the policies. LfD can address these challenges since typically it does not require expert knowledge of the dynamics. In the literature, LfD is also reported by other terms, including Programming by Demonstration (PbD), Learning by Demonstration (LbD), Assembly Plan from Observation, Learning from Observation, and Imitation Learning.

In physical human-robot interaction (pHRI), LfD aims to incorporate the knowledge and skills of humans into robots. This may enable robots to assist humans for performing collaborative tasks, including surgical simulations, driving, lifting objects, and manufacturing [4]. In such approaches, the skills could be captured from the collected data of experts movements and/or robot motions during demonstrations. Machine learning-based models are developed to learn expert skills from the demonstrations. In reproduction/practice phase, relevant information is extracted from the learning-based skill models to reproduce a taught collaborative task under unknown conditions [3,5].

In LfD, demonstrations can be provided through kinesthetic teaching and/or teleoperation [6–8]. In kinesthetic teaching, humans directly guide the robot's body to perform a task while in teleoperation, demonstrations can be done through data gloves [9], motion/vision-based systems [10], or haptic devices [6]. Kinesthetic information have been generated and measured due to a physical interaction with a robot [7,8,11] or using haptic devices in teleopration [6]. In the second part of this thesis, kinesthetic feedback is generated, however, in a surgical virtual simulation

based on a developed computed-tomography-based (CT-based) bone model. In addition, virtual fixtures have also been used in haptic-feedback-enabled simulations to improve the execution of demonstrations [12, 13]. In learning phase, the demonstrations of experts interacting with the simulation, with no virtual fixtures and/or haptic guidance, can also be used to learn motion stiffness with focus on skill assessment and residents' training/practice.

1.2 Haptic Guidance

Haptic guidance (HG) is a shared control algorithm that assists a user to complete a human-robot collaborative manipulation task [14–16]. This algorithm is typically used to guide the user along a task-specific path or restrict the motion of a tool to a range of motions [15, 17, 18]. HG can also be used to improve the performance of surgical trainees. This encourages the trainees to correct their gestures, i.e. motions or maneuvers, and improves their performance during virtual/physical training [19, 20]. Since a haptic-enabled simulator is a human-in-the-loop system, model-based HG algorithms are required to control the unpredictable and non-linear behavior of users in such pHRI [21–23]. In this thesis, proposed HG approaches are considered as a type of learning-based guidance (LbG) since HG forces are generated with respect to skill models that are learned from human demonstration in pHRI.

Skill models can be developed and used as references for HG in real time. For example, in MIS training tasks, the knowledge and experience of expert surgeons

can be incorporated into the development of HG algorithms. Surgical gestures of expert surgeons that are simple movements have been combined and sequenced to create complex skillful motions [24]. These gestures have been used to develop skill models by learning gestures from observation or by imitation [25]. Statistical models have been used to automatically segment and recognize surgical gestures. These models include generative models [26], e.g. hidden Markov models (HMMs) [24], and discriminative models [26], e.g. Conditional Random Fields (CRF) and their derivatives [27].

Impedance control proposed by Hogan [28] has been extensively used in physical pHRI to control the interaction with unknown, unstructured and dynamically changing environments. In this control method, the dynamics of a robot is described and regulated by adapting the desired parameters of stiffness, damping, and mass. In most of previous work [18–20, 29, 30], HG control gains have been selected as constant values. Furthermore, in several studies [16, 31], HG forces have adaptively been produced to assist users to perform dynamic tasks without the use of statistical models. However, in the present work, the adaptive guidance forces are continuously generated in real time using statistical models, which are developed for primitive motion (e.g. gestures) segmentation and recognition as well. Since human behavior imposes unpredictability and uncertainty in pHRI, the generation of variable guidance control gains can result in producing more precise and effective guidance force in real-time, requiring more precise human behavior modeling.

1.3 Modeling of Primitive Motions/Gestures

Primitive motions/gestures are widely represented by two classes of mathematical models [32]: dynamical systems and stochastic models. In dynamical modeling approaches, including nonlinear attractor systems and non-linear oscillators, primitive gestures are generally described by differential equations in state space. In nonlinear dynamical systems, stochastic effects such as noise and uncertainty can change the corresponding deterministic dynamics, impact the dynamics, and even change the dynamic behavior of the systems. Since the analytical models of human behavior are rarely available in pHRI applications, the non-linear, non-stationary, and non-deterministic features of stochastic/statistical models make them powerful tools for modeling human behaviors [23], including the stochastic and uncertain human behavior in terms of both mental state and resulting actions. Stochastic modeling methods enable machine learning algorithms to take advantage of a) capturing the spatial and temporal variation of the movement, b) capturing the change in variance along the movement, and c) tolerating noise and missing data.

Two types of stochastic dynamical models are usually used to represent primitive gestures: *generative* and *discriminative*. Generative models are most commonly used for both gesture recognition and the generation of a gesture prototype. However, discriminative models can only be used for gesture recognition/classification. In addition, discriminative models are unable to detect unknown gestures.

The goal of most machine learning applications is to take a vector x of input

features and predict the value of a vector y, class label. Discriminative classifiers directly model the conditional distribution $p(y|x)$ using a set of training data $\{x_n, y_n\}$. The resulting conditional distribution can be used to predict class label y for new values of x. On the other hand, generative classifiers learn a parametric model of the joint probability $p(x, y)$ and then uses this joint distribution to calculate $p(y|x)$ for selecting the most likely label y.

In order to train the classifiers, supervised machine learning algorithms require training dataset, which includes a set of initial input features and assigned labels. The generalization performance of discriminative models outperforms generative models, when labeled training set is large enough [33]. However, labeling the collected data can be expensive. Therefore, the use of generative methods is more advantageous since the training dataset is not large and rich.

1.4   Scope and Objectives

The main goal of this research is to design, develop, and examine learning-based approaches for HRI by bridging the gap between two fields: control theory and machine learning. The stochastic and unpredictable human behavior may be estimated for modeling HRI using machine learning techniques. The generation of real-time guidance forces is achieved by incorporating a motion segmentation scheme into the LbG. The LbG approaches are able to improve user performance. In these approaches, robot provides controlled forces to users for guiding them through a dynamic task

in virtual or physical environments. The scope of this research can be extended to many applications such as training and assessment, rehabilitation, and sport training to name a few.

Learning-based (haptic) guidance may be developed and used in virtual or remote environments. In the first and second parts of this thesis, LbG approaches were developed for HRI in *virtual reality* environments using haptic devices. However, in the final part of the thesis, an LbG were proposed to navigate a *remote teleoperation* robot in real world using a haptic steering and a haptic gas pedal.

The main objectives of the thesis are as follows. In the first study of the thesis, *kinematic* data as teleoperation demonstrations are used to develop statistical-based gesture models and accordingly provide LbG forces for improving user performance in a virtual environment. In the second study, which is a clinical study, the combination of virtual forces and kinematic data are used as *kinesthetic* expert surgeon demonstrations. Using the demonstrations, statistical skill models are developed to both evaluate the skill levels of users and generate LbG forces in a virtual environment. Finally, in the third study, expert demonstrations from both *kinematic* teleoperation data and *kinesthetic* teaching data are used to develop several skill models for generating guidance forces in physical environment.

The benefits of the proposed LbG approaches could be extended to other HRI application areas, including sport training and rehabilitation. The body motions of trainees are important in most sports, such as tennis, golf, baseball, and ping-pong [34, 35]. The combination of LbG in virtual environments (VEs) and motion

7

capturing systems can provide easier and more effective training for sport trainees, amateurs, or professionals. The trainees are able to interact with the VE actively by receiving guidance force via robot manipulators (haptic devices). Furthermore, LbG can be used to correct the gestures and motions of the trainees based on skill models, learned from the demonstration of athletes in that field. In other words, such training system can be used as an intelligent and automatic self-training system in various locations.

Rehabilitation allows patients, who have suffered from a stroke or different types of disabilities, to restore their functional capability to normal. In a recovery period, the activities of patients need to be continuously monitored, and subsequently corrected. The use of the proposed approaches in VEs can provide the patient with learning movement patterns [36]. Furthermore, the utilization of a motion capture system would give the patients the opportunity to compare and assess their rehabilitation task skills to the skill model of healthy persons. Thus, a healthy virtual model can be used to reduce face-to-face on-site therapy and recovery time.

1.5 Contribution of the Author

The main outcomes of the present thesis are three journal papers. The first paper has been published in the *IEEE Robotics and Automation Letters*. The second paper has been submitted to *IEEE Robotics and Automation Letters* with a conference option, the IEEE International Conference on Robotics and Automation (ICRA) 2018. The

third paper is almost ready to submit to the Advanced Robotics. The title and main technical contributions of these papers are as follows.

1. E. Zahedi, J. Dargahi, M. Kia, and M. Zadeh, "**Gesture-based adaptive haptic guidance: A comparison of discriminative and generative modeling approaches**," *IEEE Robotics and Automation Letters*, vol. 2, no. 2, pp. 10151022, 2017.

   The main contributions of this paper are to a) study the discriminative nature of Conditional Random Fields (CRF) on the improvement of HG, in comparison with HMM as a generative model, and b) provide precise real-time HG by incorporating statistical skill-based modeling into variable impedance control.

2. *The International Journal of Medical Robotics and Computer Assisted Surgery*

   Towards Skill Transfer via Learning-Based Guidance in Human-Robot Interaction: An Application to Orthopaedic Surgical Drilling Skill

   The main contributions of this work are to a) develop a kinesthetic-HRI-based approach using HCRF to both discriminate the skill levels of users and generate guidance forces in practice phase, and b) use expert demonstrations to learn motion stiffness variations that are developed based on real CT data.

3. *Advanced Robotics*

   Towards Learning-Based Guidance for Skill Transfer in Human-Robot Teleoperation

   The main contributions of this paper are to a) develop a learning-based guidance

approach for a teleoperated robot that assist operators through guidance forces delivered on haptic steering wheel and haptic gas pedal that augment to the usual force feedback of steering and pedal systems, and b) the demonstrations of expert operators are used to learn maneuvering skill models to incorporate into single-gain variable impedance control (SV-VIC) and multiple-gain variable impedance control (MV-VIC). The capabilities of these two impedance control methods for generating LbG forces are compared using several performance metrics.

1.6 Organization of the Thesis

This thesis is presented in manuscript-based format which includes three journal papers. All chapters, excluding the first and final chapters, are duplicated from the three papers that have been published in or submitted to scientific journals. The first chapter details the introduction of the LbG, a review of the literature, and rationale for the research. The final chapter discuss the conclusive remarks about the contributions of the thesis and future work.

Chapter 2

Gesture-based Adaptive Haptic Guidance: A Comparison of Discriminative and Generative Modeling Approaches

This chapter investigates the incorporation of hidden Conditional Random Fields (HCRF) as a discriminative statistical modeling technique into adaptive haptic guidance (HG) for physical human-robot interaction (pHRI). In this gesture-based HG approach, the knowledge and experience of experts are modeled to improve the unpredictable motions of novice trainees in a virtual minimally invasive surgery (MIS) training task. The HCRF models are developed for automatic gesture recognition and segmentation as well as generating guidance forces. The forces are adaptively

calculated in real time with respect to gestural similarities among user motions and the gesture models. The HCRF-based approach is compared with a hidden Markov model based (HMM-based) method for capturing the gestures of the user and providing adaptive HG. The experimental results show that the HCRF, as a discriminative method, can outperform HMM, as a generative method, in terms of user performance.

2.1   Introduction

Robots may assist humans to cooperatively perform various types of tasks that require intentional physical interactions, including lifting heavy objects, manufacturing, and surgical simulations. This aims to reduce fatigue, and increase human performance in terms of precision and speed [37].

Haptic guidance (HG) is a shared control algorithm that assists a user to complete a human-robot collaborative manipulation task [14–16]. This algorithm is typically used to guide the user along a task-specific path or restrict the motion of a tool to a range of motions [17, 18]. HG can also be used to improve the performance of minimally invasive surgery (MIS) trainees [19]. Since a haptic-enabled MIS simulator is a human-in-the-loop system, model-based HG algorithms are required to control the unpredictable and non-linear behavior of users in such physical Human-Robot Interaction (pHRI) [21–23]. In most of previous work [18, 19, 29, 30], HG control gains have been selected as constant values. Furthermore, in several studies [16, 31], HG forces have adaptively been produced to assist users to perform dynamic tasks

without the use of statistical models. In the present chapter, the adaptive guidance forces are continuously generated in real time using statistical models. The generation of variable guidance control gains can result in producing more precise and effective guidance forces in real-time, requiring more precise human behavior modeling.

Machine learning algorithms and statistical approaches take the uncertainty of robots into account to provide sound methodologies in robotics, e.g. path planning, multi-robot control, and HRI [38]. Furthermore, statistical algorithms require less accurate models compared with many classical approaches [38]. Stochastic (statistical) models are also highly effective since dynamical system models (analytical models) are not available for complex tasks [22, 39].

Surgical gestures, which are simple atomic movements, have been used to develop skill models by learning gestures from observation or by imitation [25]. In addition, statistical models have been used to automatically segment and recognize surgical gestures. These models include generative models [26], e.g. hidden Markov models (HMMs) [24] and discriminative models [26], e.g. Conditional Random Fields (CRF) and their derivatives [27]. To develop precise skill models, MIS tasks can be segmented into several gestures [24]. Kahol et al. [40] have segmented an MIS task into several surgical gestures to discriminate MIS skills. Reiley and Hager [24] have developed HMMs based on surgical gestures (surgemes) to evaluate MIS skills. The developed HMMs in previous studies have mainly been used in off-line MIS skill assessment, which are not applicable for real-time haptic rendering.

In this study, HCRF is employed as the discriminative counterpart of HMM. This

13

modeling technique is an extension of CRF that incorporates hidden states for modeling the underlying structure of the observations. For classification purposes, discriminative approaches directly build the conditional probability distribution, which is more related to the classification boundary. The generative approaches learn one model for each class and model a distribution over observations. HCRFs have successfully been used for classification applications, including gesture recognition [41,42] and speech recognition [43]. Although generative models, e.g. HMM, have been utilized for HG applications, discriminative models, specifically HCRFs, have not been used to provide HG in pHRI.

This chapter presents a new adaptive statistical gesture-based HG approach, in which a robot applies controlled forces on the hands of a user to guide him/her through a virtual task (details in Section 2.3). The aim of the present work is two-fold. In the first study (presents in Section 2.4), the gesture-based approach is initially examined for generating real-time adaptive HG and its effects on user performance. Then, in the second study (describes in 2.5), the efficacy of the HCRF-based HG approach is investigated by designing a relatively more complex task. The results also compare with no HG, constant HG, and HMM-based HG. To make the task more complex, it is created by considering variable sizes and sequence of gestures.

The main contribution of the present study is to incorporate the discriminative nature of CRF into gesture-based HG in pHRI. The capabilities of discriminative and generative models for generating HG are compared using several performance metrics. The conclusive remarks about the contribution and our main goals are presented in

Section 2.6.

2.2 Haptic Guidance and Modeling of Gestures

HG provides forces to users when they perform a visuo-motor learning task [15]. In other words, a haptic interface provides the users with physical guidance and gives them the kinesthetic understanding of the required motion for performing a desired motion [44]. Several studies have indicated the efficiency of such an approach in learning movements using virtual training simulators [44–46]. The following section provides the required information regarding the modeling of gestures that is an essential part of the HG approach.

2.2.1 Modeling of Gestures

Gestures can be represented by mathematical models, including dynamical system models and stochastic models [32]. The non-linear, non-stationary, and non-deterministic features of stochastic/statistical models make them useful tools for modeling the stochastic and uncertain human behaviors [19, 22, 23]. Stochastic modeling methods enable machine learning algorithms to take advantage of a) capturing the spatial and temporal variations of the movement, b) capturing the change in the variance along the movement, and c) tolerating noise and missing data.

Several researchers [19, 24, 40, 47–49] have used HMMs, as generative models, to develop MIS task models. Two main weakness of using generative models have been

reported in the literature [33, 41, 50]: 1- For the sake of simplicity, observations are assumed to be conditionally independent. It is often difficult to accommodate long-term dependencies among observations or rich overlapping features of the observation at multiple time steps and 2- Hidden states maximize the likelihood of generating all the examples of a given gesture class, but the likelihood is not certainly optimal for the discrimination of gestures. Our focus is on using HCRF for providing HG and comparing it with HMMs.

2.2.2   Performance Metrics

The evaluation methods used in this study and created virtual environments (VEs) are based on a peg transfer task, which is a fundamental of laparoscopic surgery (FLS) task. In this task, the goal is to transfer six blocks using two curved Maryland graspers in minimum time with minimal errors, from one side to another and back again. Many MIS objective evaluation metrics have been proposed to measure user performance [49, 51, 52]. Four quantitative performance metrics are used in this study:

1- Completion Time (T): This is the total time required for each task to be completed.

2- Path Length: It is the length of the path traversed by the end-effector over time.

3- Normalized Motion Smoothness (N-MS): This metric is a factor related to the instantaneous jerk defined as $j = \frac{d^3x}{dt^3}$ (cm/s^3) and represents a change in

acceleration. N-MS is calculated as follows [52].

$$N - MS = 1 - \frac{1}{T}\sqrt{\frac{1}{2}\int_0^T j^2 dt}. \tag{1}$$

The acceleration data and MS are normalized in a range of 0 through 1 to ease the interpretation of this metric [51].

The shorter task completion time, the shorter path length, and the higher motion smoothness represent a better performance [19, 51, 52]. In addition to these metrics, we use another evaluation metric to further investigate the effects of the HG:

4- Average Angular Error (AAE): This is the average difference between the angles of desired and current gestures:

$$AAE = \frac{1}{N}\sum_{i=1}^{N}|\alpha_i|, -180 \leq \alpha_i < 180, \tag{2}$$

where α_i is the angular error between the tangent vector to the path of user motion and the direction of desired gesture at i time step, and N is the number of time steps.

AAE represents how well HG encourages users to correct their gestures by evaluating the direction/angle of a performed gesture, regardless of the distance between end-effector and reference gestures. Lower AAE represents better performance.

17

2.3 Gesture-Based Variable Impedance HG

This section presents the details of the approach that uses the gestural differences as the sources of the disagreements between human and robot to produce adaptive HG.

2.3.1 General Architecture

The proposed approach includes: 1) developing continuous HMM and/or HCRF models for the kinematic observations associated with each reference gesture which is an off-line process, and 2) generating variable control gains in real time based on the similarity between the current gesture of user and a modeled gesture. The dynamics of the robot is described by

$$f_h + f_{hg} = M\ddot{\boldsymbol{x}} + D\dot{\boldsymbol{x}} \tag{3}$$

where $\boldsymbol{x}$ is the position of the end-effector, and M and D are positive-definite matrices representing inertia and damping, respectively. As shown in Fig. 1, the two inputs to the mass-damper dynamics are human applied force (f_h) and additional virtual force (f_{hg}), which represents variable guidance force.
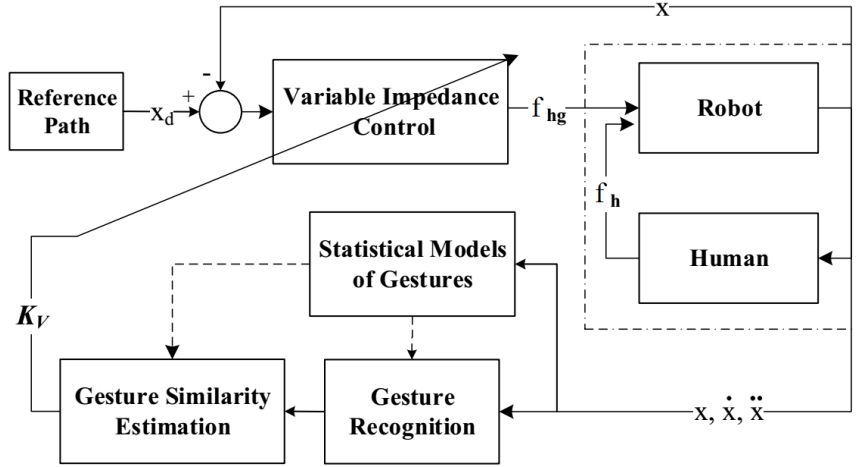
Figure 1: The schematic diagram of the adaptive gesture-based HG approach. Human and robot collaborate to perform a virtual task. Gesture Recognition block, which is connected to the trained Statistical Models of Gestures (HMMs/HCRF), recognizes and segments user motions. Gesture Similarity Estimation generates a variable stiffness gain (K_V) based on the similarities among current user gestures and trained (reference) models. The Variable Haptic Guidance calculates forces to guide the user through a reference path. $x, \dot{x}, \ddot{x}$ are position, velocity, and acceleration of the robot/human, respectively.

Fig. 1 shows the architecture of the HG approach. During task execution, the motion of a user is segmented into gestures. Then, gesture similarity estimation block determines how well the current gesture of the user is similar to the corresponding gesture model. The result is the value of variable stiffness gain (K_V) in our impedance control strategy (variable impedance control block) to produce the guidance force. In this approach, when a user moves the end-effector less similar to a reference gesture model, greater guidance forces are applied to the end-effector and user's hand; this encourages the user to perform the correct gesture.

2.3.2 Gesture Recognition

HMM-based

We develope continuous HMMs with Gaussian mixture distribution for gestures of an MIS type training task. A K-state $\{S_1, S_2, ..., S_K\}$ continuous HMM with a Gaussian observation, $\lambda = (A, B, \pi)$, is defined by three parameters [53]: a state transition probability distribution $A = \{a_{ij}\} = P(S_t = j \mid S_{t-1} = i)$, a set of observation model probabilities $B = P(O_t|S_t)$, and a set of prior probabilities $\pi = \pi_i$, where $\pi_i = P(S_1 = i)$ and $1 \leq i, j \leq K$.

Since the actual observation sequence is continuous, generating a continuous output requires estimating the probability density function (pdf) of the state output (observation model). To model this density, a set of training data is used to estimate the Gaussian mixture parameters. The M-mixture of observation model is defined as follows.

$$P(O_t = o|S_t = i) = \sum_{m=1}^{M} P(M_t = m|S_t = i)\mathcal{N}(o; \mu_{m,i}, \Sigma_{m,i}) \tag{4}$$

where $\mathcal{N}(o; \mu, \Sigma)$ is the Gaussian density, μ_i and Σ_i are the mean and covariance of the state i, O_t is the observation, S_t is the state, M_t is a hidden variable that specifies which mixture component to use, and $P(M_t = m|S_t = i) = c(i, m)$ is the conditional coefficient of each mixture component.

In order to train HMMs, the model parameters are optimized to maximize $P(O \mid$

λ), where O is an observation sequence. An expectation maximization (EM) algorithm called Baum-Welch is used to establish maximum likelihood (ML) parameter estimation for HMMs [53].

HCRF-based

The goal of most machine learning applications is to take a vector o of input features and predict the value of a vector y, class label [33]. Discriminative classifiers directly model the conditional distribution $p(y|o)$ using a set of training data $\{o_n, y_n\}$. The resulting conditional distribution can be used to predict class label y for new values of o. CRFs avoid the independence assumption between observations, and can incorporate both long-term dependencies and overlapping features into the model. CRFs use a probability distribution to model the entire sequence of labels, given the entire observation sequence.

HCRF models incorporate hidden state variables in a discriminative multi-class random field model to provide a way to determine a single label for an entire input sequence, e.g. the gesture of users. An HCRF model is defined by [41]:

$$P(y|O, \theta) = \sum_S P(y, S|O, \theta) = \frac{\sum_S e^{\psi(y,S,O;\theta)}}{\sum_{y' \in Y, S \in S^m} e^{\psi(y',S,O;\theta)}}, \tag{5}$$

where $y \in Y$ is a class label, O is an observation sequence, S is the set of hidden states, and θ is the model parameters. $\psi(y, S, O; \theta)$, parametrized by θ, calculates the compatibility among a label, a set of observations and hidden states. The following

objective function is used for estimating the parameters [41]:

$$L(\theta) = \sum_{i=1}^{n} logP(y_i|o_i, \theta)) - \frac{1}{2\sigma^2} \|\theta\|^2 , \tag{6}$$

where $\{y_i, o_i\}$ is the training set of labeled examples, n is the number of training sequence data, and σ^2 is variance of a Gaussian prior. In this work, a Quasi-Newton optimization method, L-BFGS [54], is used to find optimal parameter values ($\theta^* =$ arg max$_\theta$ $L(\theta)$).

2.3.3   Gesture Similarity Estimation

HMM-based

HMM-based similarities are calculated to compare the gestures of users and reference models in real time. Our method continuously calculates gestural similarity (GS) according to the maximum log-likelihood of the observation sequence:

$$GS = \arg \max_{j} \ log \ P(O|\lambda_j) \tag{7}$$

where $O = \{o_{t-nT}, o_{t-(n-1)T}, ..., o_t\}$ is the last n observation sequence with the sampling time T, λ_j is an HMM that models a gesture, $1 \le j \le l$ while l is the number of trained gestures, and the observation o_t is a vector of the features $(x, \dot{x}, \ddot{x})$ at time t.

$P(O|\lambda_j)$ is the probability that shows the similarity between the current and modeled gesture. This similarity determines the impedance control gain, increasing in the probability leads to decreasing the gain. As a result, smaller gains let the user to move the end-effector with less guidance.

HCRF-based

In real time, the proposed HCRF-based HG approach recognizes gestures and continuously generates gestural similarity (GS) between the user motion and the trained HCRF:

$$GS = \arg\max_{y \in Y} \; log \; P(y|O, \theta^*) \tag{8}$$

where O is the last n observation sequence of user motion and $Y = \{y_1, y_2, ...y_l\}$ is the set of labels (trained gestures).

2.3.4 Variable Impedance Control

A variable impedance control scheme is used to lessen the effects of unmodeled dynamics, including unobserved deviations from a motion plan, and natural variability of human behavior. Forces are calculated using the following equation:

$$f_{hg} = -K_V(\boldsymbol{x} - \boldsymbol{x}_d) \tag{9}$$

where f_{hg} is the guidance force, $K_V > 0$ is a scalar variable stiffness gain that is a function of gestural similarity (GS), $\boldsymbol{x}_d$ is the desired position on the reference path, and $\boldsymbol{x}$ is the current position of the end-effector. The desired position, which is closest to x, is instantaneously found based on computational geometry methods [55].

A linear modulation function is selected for K_V that relates each calculated gestural similarity to a stiffness gain:

$$K_V = \frac{K_{max} - K_{min}}{GS_{min} - GS_{max}}(GS - GS_{max}) + K_{min}, \tag{10}$$

where $K_{min} \leq K_V \leq K_{max}$ and $GS_{min} \leq GS \leq GS_{max}$. In this work, the domain and range of this function are limited to $[GS_{min}, GS_{max}]=[-400, 0]$ and $[K_{min}, K_{max}]=[0, 222\ N/m]$, respectively. GS_{min} was selected based on the results of a pretest user study, in which the objective was achieving a minimum gesture recognition error rate. This study also indicated that in the operation area of the system, the linear modulation is a fair mapping between GS and K_V to encourage users performing correct gestures. As presented in (7) and (17), the stiffness gains are adaptively determined in real time according to the gestures of the user's hand/tool.

A three-point moving average filter of previous stiffness gain data is used to smooth the stiffness gains and accordingly the guidance forces. The number of points is experimentally selected to obtain a smooth output signal.

2.4 Experiment 1: Evaluation of Model-based HG

The goals of the first experiment are to examine the gesture-based approach and compare user performance for adaptive HG, constant HG and no HG conditions. The second experiment on the incorporation of HCRF for providing adaptive HG is presented in Section 2.5.

2.4.1 Experimental Setup

Fig. 2 shows the experimental setup that includes an MIS tool, Phantom Omni haptic device, male torso mannequin, and virtual environment (VE). The tool is attached to the haptic device that is set up on a movable and height adjustable table. The device records the motion of the tool and provides HG to the subjects. It is a 6 degree-of-freedom (DOF) robot manipulator and is capable of exerting force feedback in 3 DOF translational motions. The sampling frequency for capturing data is 50 Hz and the variable gain is updated every 20 ms.
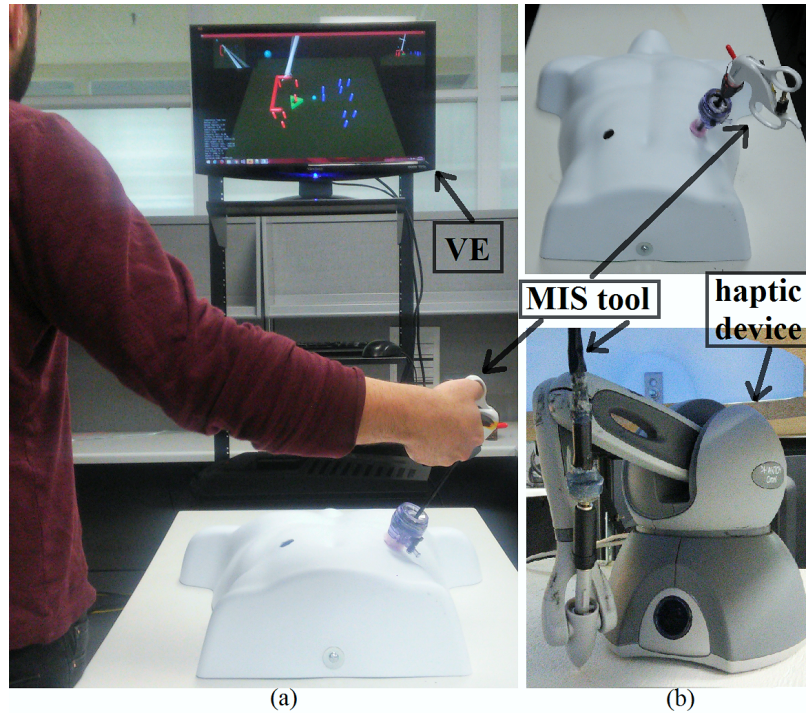
Figure 2: Experimental setup: (a) A user is tracing a predefined path in the VE using the MIS tool. (b) The tool (grasper) is attached to a haptic device. The device applies the guidance forces on the user's hand via the tool.

According to previous studies of stability of haptic interaction [56,57], the coupling of the Phantom 1.0 haptic device and a VE is locally stable while the designated stiffness gains keep below 1015 N/m [56]. In our study, although using a different version of Phantom device, we selected a lower range of stiffness in the range $0 - 222N/m$, that was experimentally verified to lead to a stable haptic interaction.

Two MIS related tasks are designed in the VE for experimental evaluation. The tasks involves moving the end-effector and carrying an object (hollow triangle) in the VE from a peg to another peg with respect to a predefined sequence. Before each experiment, the subjects were guided to perform the tasks and instructed to complete the tasks precisely as quickly as possible. Every subject had five minutes

to get familiar with the setup.

2.4.2   Training Gestures: Generative Models

HMM models: Four MIS gestures in 3D space, including *right, up, left* and *down*, are selected and an HMM is trained as reference gesture model for each. The four models are λ_r, λ_u, λ_l, and λ_d that indicate the end-effector movement is along x-axis, along y-axis, along the negative x-axis, and along the negative y-axis, respectively.

A data set was gathered from nine users who interacted with the haptic device and performed each basic gesture ten times using the experimental setup, while no HG is provided. The users worked with the experimental setup at least 10 hours and practiced designated gestures many times. Thus, the training data set was collected from the users who are experts in performing the gestures, compared with new users. The velocity and acceleration were derived from the position of the end effector. After the data collection, the data was segmented and sorted into the gesture groups. The HMMs were developed with 15 states, a mixture of two continuous Gaussian probability distributions, and a recognition/classification accuracy of 88.5%. The accuracy was calculated using confusion matrix parameters, including true positives (TP), false positives (FP), true negatives (TN), and false negatives (FN) [50]:

$$\text{Recognition Accuracy} = \frac{TP + TN}{TP + FP + FN + TN} \tag{11}$$

The length of observation (window size), which was used to compute the gestural similarity (GS) in real time, was five data points. Bakis (left-to-right) topology [53] was used for developing the HMMs because this topology efficiently describes the sequential nature of motions. The number of Gaussian mixtures and hidden states were determined by minimizing the classification error rate on the training data.

2.4.3 Procedure

Sixteen healthy male and right-handed subjects (aged 20 to 28 with a mean age of 23.2 years) were asked to complete a task, which was tracing a predefined virtual path above four pegs using the MIS tool. The path was square-shaped and composed of four same-size gestures. The sequence of gestures was $\{down, right, up, left\}$. Every subject performed the task in the following modes.

HMM-based Haptic Guidance (HMM-HG): Our proposed HG approach was used to guide subjects through the task. The stiffness gain range is limited to $0 - 222\ N/m$ for the safety of haptic device. Choosing this range can give the subjects a good sense of the path they should follow, but they are able to stay outside the reference path, if necessary.

Haptic Guidance with Constant Stiffness (CS-HG): A constant gain ($K = 118\ N/m$) was selected that showed the best performance during a preliminary experiment among four tested gains ($K = 44\ N/m$, $K = 118\ N/m$, $K = 166\ N/m$, and $K = 222\ N/m$).

No Haptic Guidance (NHG): No HG was provided.

2.4.4 Results and Discussion

The means and standard errors for the completion time, path length, and motion smoothness across all subjects are presented in Fig. 3. Several trends are evident in the data. The results show when there is no HG, subjects have smoother movements with a relatively higher path length and spend more time for completing the task. However, HG (for both HMM-HG and CS-HG modes) improves user performance in terms of reducing the completion time and path length, compared with NHG. A similar trend has also been reported in Li and Okamuras' study [29] when subjects performed a curve following task. Safavi et al. [19] have also reported a similar trade-off between the completion time and motion smoothness for following a sequence of motions.
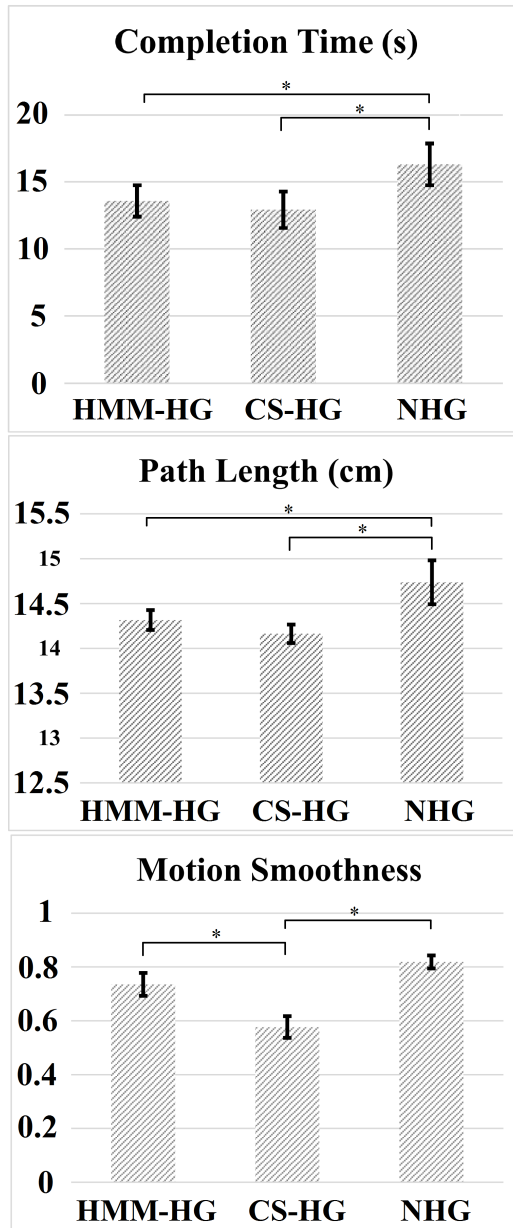
Figure 3: The means and standard errors across all subjects for three modes (HMM-HG, CS-HG, and NHG). Both HG methods (HMM-HG and CS-HG) decrease the task completion time and path length at the cost of decreasing the motion smoothness. The proposed approach (HMM-HG) improves the motion smoothness significantly, compared to CS-HG. * shows significant differences with $P < 0.05$.

The results for the gesture-based HG (HMM-HG) shows better performance in balancing between the completion time and motion smoothness among the three

methods. Both HG methods decreases the completion time and path length. However, HMM-HG shows a better motion smoothness in comparison with the CS-HG. As presented in Table 1, the results of a repeated measures analysis of variance (ANOVA) significantly supports the trends in the data. There are statistically significant differences for three metrics among HMM-HG, CS-HG, and NHG modes. Thus, Bonferroni post-hoc analysis is conducted to examine statistically differences between pairwise measured performance metrics. In Fig. 3, * indicates significant differences with $P < 0.05$.

Table 1: The results of ANOVA for the first experiment. 0.05 is the rejection level.

	Completion Time	Path Length	Motion Smoothness
F(2, 30)	6.69	11.01	11.24
P-value	0.003	0.0002	< 0.0001

2.5 Experiment 2: Evaluation of Discriminative-based HG Versus Generative-based HG

To our best knowledge, for the first time in this chapter, an HCRF, as a discriminative model, is used to generate adaptive HG. The results from Section 2.4 indicate that providing adaptive HG using generative models is a promising approach to improve user performance. However, the approach only improves motion smoothness in comparison with constant HG method. The second experiment was conducted to

investigate the approach using an HCRF-based HG with a relatively more complex task.

2.5.1 Training Gestures: Discriminative Models

HCRF model: A single HCRF, with 15 hidden states and a recognition accuracy of 92.1%, was trained for six gestures: $Y = \{right, up, left, down, in, out\}$. The training data was the same and the number of states was selected by minimizing the classification error rate on training data. The accuracy was computed using (11).

2.5.2 Procedure

Eighteen healthy male right-handed students (aged 22 to 31 with a mean age of 25.6 years) participated in this experiment. The subjects were completely different from the subjects of the first experiment. Fig. 4 shows the MIS-type task with several pegs that were randomly deployed on the peg board. Subjects were asked to lift a triangular object with the MIS tool from the top right peg, carry the object, maneuver above the pegs, and put the object down onto another peg. The task was composed of several gestures with various sizes. Every subject carried out this task in three previous modes (HMM-HG, CS-HG, NHG described in Subsection 2.4.3) and:

HCRF-based Haptic Guidance (HCRF-HG): The developed HCRF model is used to provide adaptive HG.
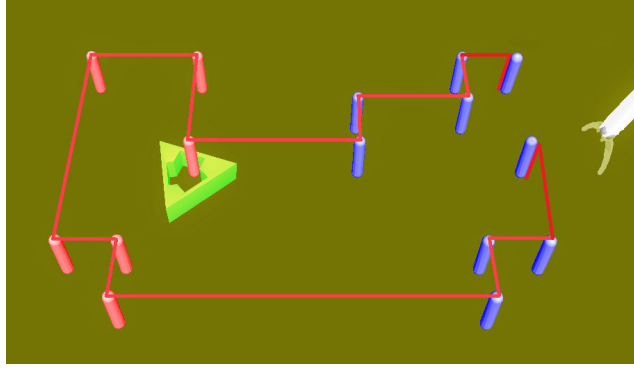
Figure 4: The designed MIS virtual task for the second experiment.

2.5.3 Results and Discussion

The means and standard errors across all subjects are shown in Fig. 5 for four conditions: HMM-HG, CS-HG, NHG, and HCRF-HG. Table 2 shows the repeated measures ANOVA results, with a rejection level of 0.05. The results of post-hoc Bonferroni pairwise comparisons, $^*(P < 0.05)$, are shown in Fig. 5.

There are several trends in the results. HCRF-HG, as a discriminative approach, shows the best overall performance by encouraging the subjects to perform the most correct gestures smoothly. Among all the methods, HCRF-HG and CS-HG show better performance improvement in terms of path length, completion time, and AAE. HCRF-HG also shows a better motion smoothness compared to CS-HG. NHG only provides better motion smoothness, which is also observed in the several studies in the literature [19, 29] and the first experiment.
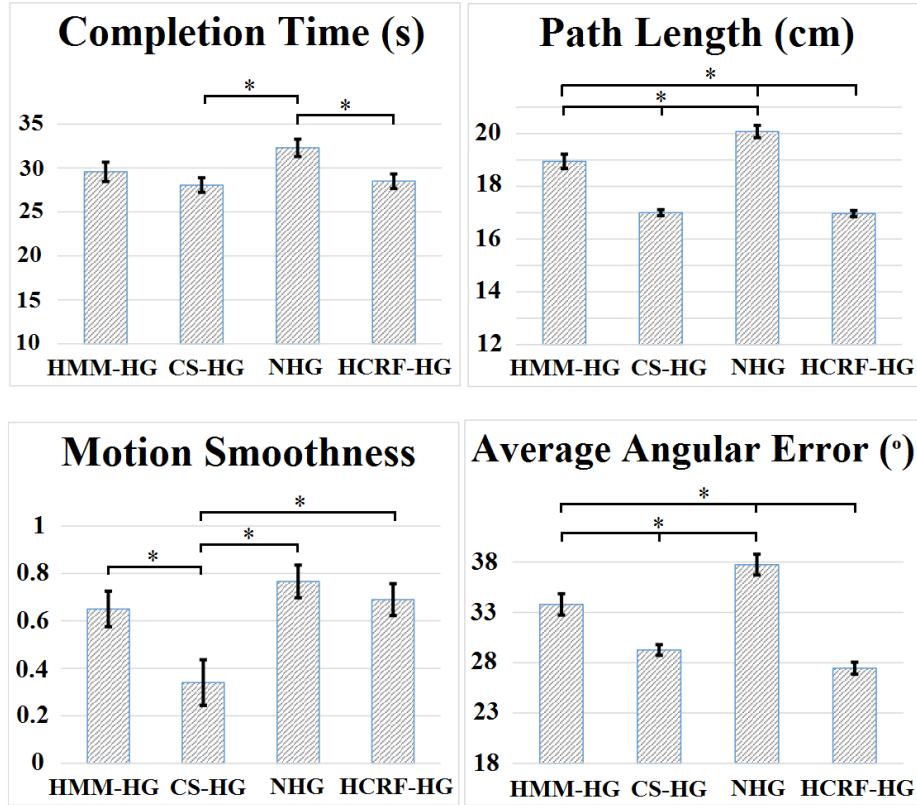
Figure 5: The means and standard errors of the performance metrics across the subjects of the second experiment for four modes (HMM-HG, CS-HG, NHG, and HCRF-HG). HCRF-HG approach provides better performance improvement overall. * marks significant differences.

Table 2: The ANOVA results for four performance metrics.

	Completion Time	Path Length	Motion Smoothness	AAE
F(3,51)	11.29	59.96	5.38	21.89
P-value	<0.001	<0.001	0.002	<0.001

The results show that between the generative and discriminative HG approaches, the latter is further capable of improving the user performance. Path length (a

metric related to position error) and AAE (angular error), for HCRF-HG are significantly better than for HHM-HG. While for completion time and motion smoothness, the Bonferroni post-hoc test found no significant differences between HCRF-HG and HMM-HG.

The gesture recognition accuracies of modeling methods have commonly been used in the literature [27, 41, 58] to compare the performance of the methods. Our results also indicate the higher accuracy, the higher user performance, however, in a different scale. For example, as reported in Subsections 2.4.2 and 2.5.1, the recognition accuracy of the HMM and HCRF models are 88.5% and 92.1%, respectively. Although the accuracy improvement is about 4%, HCRF-HG results in over 11% and 23% improvement in path length and AAE, respectively, in comparison to HMM-HG.

It seems from the results that HCRF recognizes the gesture label that better corresponds to a time slice sequence. In real-time HG, statistical models should be capable of recognizing and segmenting the motion of users only based on the time slice of observation sequence. The gestures are usually performed at various timescales and may show dependencies. HCRF further captures these temporal dependencies among observations, compared to HMM. The better real-time gesture recognition results in the more precise calculation of the GS and resulting HG forces. Thus, HCRF-HG is better suited for a HG task, compared with HMM-HG.

A benefit of adaptive HG over constant HG is also noticed by comparing the results of motion smoothness of the two experiments. From the first experiment to the second experiment, motion smoothness considerably decreases from 0.57 to 0.33

(24%) for CS-HG. However, motion smoothness slightly decreases from 0.81 and 0.73 to 0.76 and 0.65 for NHG and HMM-HG, respectively. It seems that even though the task of the second experiment is more complex than the first task, adaptive HG (HMM-based approach) is able to adjust control gains for achieving smoother motions. Furthermore, the selected constant gain (K) of the first experiment might not necessarily be optimal for the second experiment. The trial and error method should be used to tune the constant gain for every new task. However, the gesture models (HMMs) of the first experiment are precisely used in the second experiment. These models are readily usable to provide HG for new tasks.

To analyze the performance of our HG approach in regard to task complexity, a two-way ANOVA is conducted on the data of the two experiments. Table 3 presents the effects of task complexity (TC) and HG factors on user performance. The TC has two levels (Low in the first experiment, and Medium in the second one) and HG has the three common modes between the experiments (HMM-HG, CS-HG, and NHG). We can independently analyze the effects of TC for completion time and motion smoothness because there is no statistically significant interaction between the two factors. However, for path length, we cannot look at the effects of TC, independently, since there is a significant interaction.

Table 3: The two-way ANOVA results, the effects of task complexity (TC) and HG modes on user performance.

	Time	Path Length	Motion Smoothness
F(1,15)-TC	58.22	583.62	8.83
P-value	<0.0001	<0.0001	0.006
F(2,30)-HG modes	21.09	65.28	14.5
P-value	<0.0001	<0.0001	<0.0001
F(2,30)-interaction	0.34	33.89	1.15
P-value	0.71	<0.0001	0.32

Table 4 presents the results of a Tukey-Kramer post-hoc test on the effects of TC on completion time and motion smoothness for various HG modes. The results confirm the trend in the graphs that completion time is obviously higher for the Medium TC than for the Low TC in all HG and NHG modes. In other words, subjects spent more time to complete the second task because it is composed of more steps and gestures as well as longer path length. However, the results only show a statistically significant difference for CS-HG mode, suggesting that it was more difficult for subjects to smoothly complete the more complex task in CS-HG mode compared with when they completed the task in HMM-HG.

Table 4: Results of pairwise comparisons of task complexity levels.

	Completion Time		Motion Smoothness	
Comparison	F(1,17)	P	F(1,17)	P
HMM-Med & HMM-Low	93.43	<0.001	2.23	0.14
CS-Med & CS-Low	79.99	<0.001	5.85	0.02
NHG-Med & NHG-Low	62.28	<0.001	1.14	0.29

2.6 Conclusions and Future Work

This chapter proposes an adaptive haptic guidance (HG) approach based on a discriminative model (HCRF) for human-robot interaction. We have segmented a task into gestures for modeling purposes and provided guidance forces to the user via a robot manipulator. Due to the human stochastic behavior and the sequential nature of the tasks, we have developed statistical models (HMMs and HCRF) to generate variable controlled forces according to the gestural differences. The stiffness gains have been adjusted in real time when there is a gestural disagreement between the user and the modeled gestures. The gesture-based variable impedance approach has enabled subjects to complete a task with better performance while balancing between completion time, motion smoothness, and average angular error, compared with no HG and constant HG conditions.

The results fairly confirm that the utilization of discriminative approach compared to generative approach for providing adaptive HG is promising to improve user

performance for completing dynamic tasks. There is no linear mapping between the recognition accuracy of the statistical gesture models and the performance outcomes of the HG approaches. Since human is involved in the HG control loop, extensive human factor studies are required to discover the parameters that may affect the outcomes of such haptic-enabled systems in pHRI.

To train statistical models, features should be selected in regard to the characteristics of the gestures. Since in this chapter, the gestures are tool tip movements in orthogonal direction, the linear position, velocity and acceleration of the tool tip are chosen as features. To train more complex gestures, including positioning needle, making C loop, and pulling suture, other kinematic variables, including the rotational velocity and rotation matrix of the tool tip, as well as video data may be added to the features. This facilitates the recognition of complexed gestures and consequently the calculation of effective HG forces.

In our future work, the proposed approach will be investigated by expanding the reference models with more gestures and adding adaptive damping gains to the variable stiffness control strategy.

Chapter 3

Towards Skill Transfer via Learning-Based Guidance in Human-Robot Interaction: An Application to Orthopaedic Surgical Drilling Skill

This chapter presents a machine learning-based guidance (LbG) approach for kinesthetic human-robot interaction (HRI) that can be used in virtual training simulations. Demonstrated positional and force skills are learned to both discriminate the skill levels of users and produce LbG forces. Force information is obtained from virtual forces, which developed based on real computed tomography (CT) data, rather than force

sensors. A femur bone drilling simulation is developed to provide a practice environment for orthopaedic residents. The residents are provided with haptic feedback that enable them to feel the variable stiffness of bone layers. The X-ray views of the bone are also presented to them for better tracking of a pre-defined path inside the bone. The simulation is capable of planning a drill path, generating X-rays based on user defined orientation, and recording motion data for user assessment and skill modeling. The knowledge of expert surgeons is also incorporated into the simulation to provide LbG forces for improving the unpredictable motions of the residents. To discriminate the skill level of users, machine learning tools are used to develop surgical expert and resident models. In addition, to improve residents performance, the expert HCRF is used to generate adaptive LbG forces regarding the similarities between residents motions and the expert model. Experimental results show that the learning-based approach is able to assess the skill of users and improve residents performance.

3.1   Introduction

Osteoporosis is one of the most common causes for hip fracture, leading to the increase of fracture risk [59]. Even in the developed world, 2% to 8% of males and 9% to 38% of females are diagnosed with osteoporosis [60]. No cure has been developed for osteoporosis, but with proper treatment, the bone loss can be slowed. Since it shows next to no symptoms, most patients do no seek medical attention until bone fracture occurs. Hip fracture is a serious medical issue with a high mortality rate of between

20% and 35% within one year of fractured femur [61, 62].

In osteosynthesis treatment, the surgeons can reposition the dislocated bone fragments into an acceptable position in a non-invasive manner, and apply nails as fixtures. These procedures are guided by real-time x-ray images. Since the surgeon has to determine the depth of the drill by experience, catastrophic results could occur. Thus, developing the intuition for the operation before the surgery is crucial to the success of the operation. This requires excessive practice, which is costly.

Surgical simulations provide a safe environment in which a surgeon may repeatedly practice a procedure without impacting patient safety [63]. The simulations could steepen the initial learning curve and facilitate the transfer of obtained skill to the real clinical environment [64]. Virtual reality (VR) training systems also can serve as safe and effective alternatives to more traditional learning venues, such as the clinical operating room (OR) [65].

Training simulators are human-robot interaction (HRI) systems in which robots may assist users to complete a human-robot collaborative manipulation task. Since such systems are human-in-the-loop systems, skill models can be developed and used as references for haptic guidance force calculation in real time. This encourages trainees to correct their motions and improve their performance based on the skill models [4]. Statistical models, e.g. hidden Markov models (HMMs) and their derivatives, have been used to develop surgical skill models for discriminating and evaluating the skill levels of users [24, 49, 51, 66]. Using statistical models and machine learning algorithms, the uncertainty of robots and environments are considered for providing

sound methodologies in robotics. Statistical models are also highly effective when analytical models are rarely available for complex tasks [22, 39]. In [4], using statistical models, a *kinematic* (positional) learning-based approach has been proposed to generate only guidance forces. However, in the present work a *kinesthetic* (positional and force) learning-based approach is developed for generating guidance forces as well as skill assessment in a virtual surgical simulation.

In HRI, learning from demonstration (LfD) aims to incorporate the knowledge or skills of humans into robot learning [6]. This may enable robots to assist humans for performing collaborative tasks, including lifting objects, manufacturing, and surgical simulations [4]. Demonstrations can be provided through kinesthetic teaching and/or teleoperation [6–8]. In kinesthetic teaching, humans directly guide the robot's body to perform a task while in teleoperation, demonstrations can be done through data gloves [9], motion/vision-based systems [10], or haptic devices [6]. Kinesthetic information have been generated and measured due to a physical interaction with a robot [7, 8, 11] or using haptic devices in teleopration [6]. Similarly, we generate kinesthetic feedback, however, in a surgical virtual simulation based on a developed computed-tomography-based (CT-based) bone model. In addition, virtual fixtures have also been used in haptic-feedback-enabled simulations to improve the execution of demonstrations [12, 13]. On the contrary, in our learning phase (detailed in Section 3.3), the demonstrations of experts interacting with the simulation, with no virtual fixtures and/or haptic guidance, are used to learn motion stiffness with focus on skill assessment and residents' training/practice.

In the literature, both positional and force data have been used to teach a robot collaborative skills from demonstrations [6, 7, 67, 68]. In orthopedic drilling surgery, since bone tissues have different stiffness, expert surgeons should apply controlled and precise force to each layer of the bone in order to avoid damaging bone tissues. In such applications, the control of interaction force is required to establish an appropriate relationship between applied force by the human/robot and changes in the kinematic state of the contact point with the environment. In contrast to previous work which use expensive force/torque sensors to obtain force skills, we use virtual interaction force to capture force skills for teaching a robot collaborative skills and controlling the interaction force.

In this chapter, we propose a learning-based approach in kinesthetic HRI simulation that aims to transfer the skills of expert surgeons to resident trainees (see Fig. 6). During learning phase, the expert demonstrations are used to develop an expert HCRF model for learning the stiffness variations of different bone layers. In addition to the expert HCRF, a novice HCRF model is also developed from the demonstration of novice residents to discriminate the skill levels of a new user. In practice phase, the learning-based approach, which encoded the stiffness variations, guides the trainees to perform training tasks similar to the experts motions.
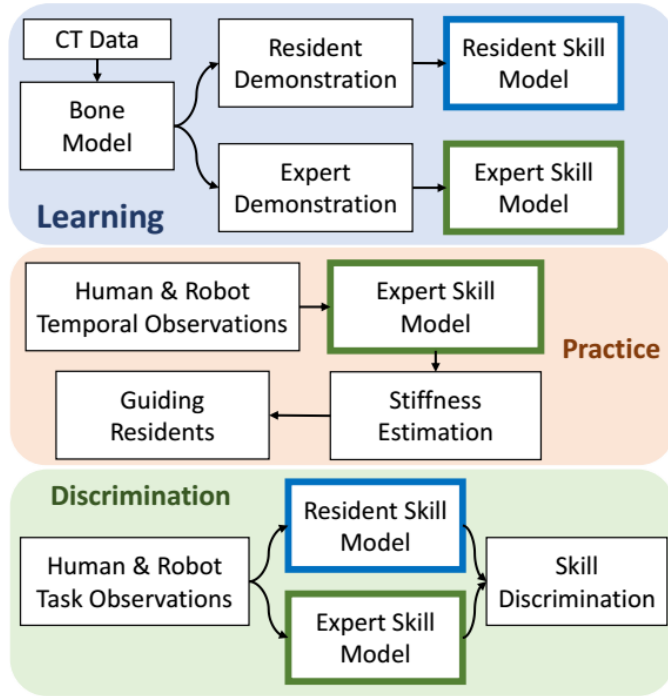
Figure 6: Phases of the proposed approach. Learning: use expert and resident demonstrations to develop skill models (HCRFs). Practice: produce real-time learning-based guidance forces to adapt the motion stiffness of residents according to the interaction provided by the experts. Discrimination: assess and discriminate the skill level of user.

To investigate our approach, we develop a simulation for femoral bone drilling, with applications to osteonecrosis and fracture stabilization (presented in Section 3.4). We develop procedures to a) model patient-specific 3D bones from CT scan data, b) incorporate density and stiffness properties into the models for more realistic demonstrations, and c) evaluate residents performance. Our approach is evaluated experimentally, which is detailed in Section 3.5.

The main contributions of the present work are to a) develop a kinesthetic-HRI-based approach to both discriminate the skill levels of users and generate guidance forces for a virtual surgical simulator, and b) use virtual haptic rendering forces, which are developed based on real CT data, to learn motion stiffness variations.
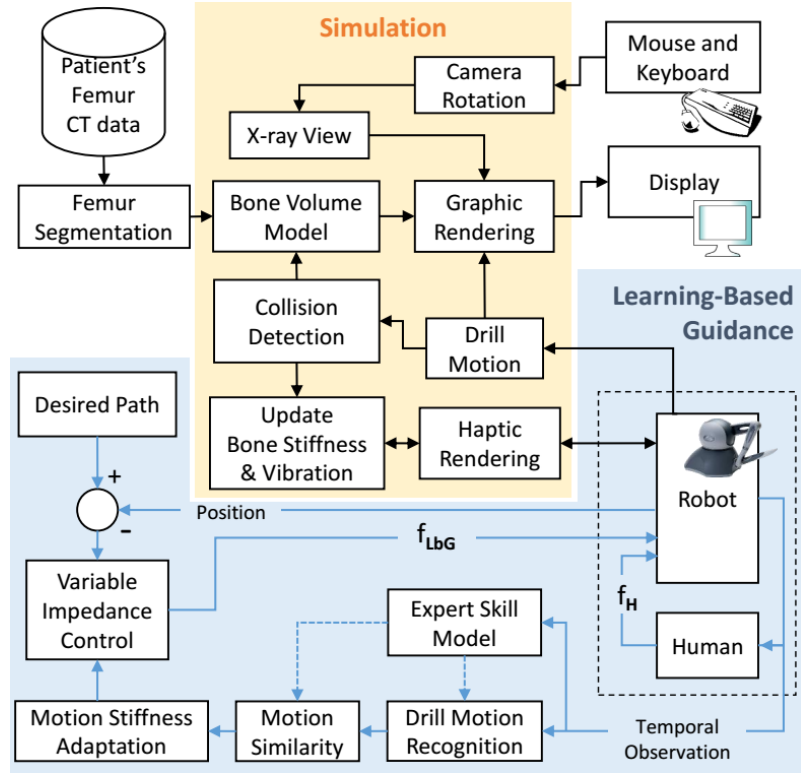
Figure 7: General architecture of the simulation and the learning-based guidance (LbG) approach. Expert skill model is used to recognize and segment the drilling motion within the bone layers. Motion similarity generates adaptive stiffness gains (K_{LbG}) based on the similarities among current drilling motion and the reference skill model. A variable impedance control strategy calculates forces to guide the user through a reference path. Temporal observations are position, velocity, and acceleration of the robot/human in addition to haptic rendering force.

3.2 General Architecture

The general architecture of the simulation and the learning-based approach is shown in Fig. 7. In LbG, during practice, the expert skill model (HCRF) segments the drilling motion of users within the bone layers. Then, motion similarity estimation block determines how well the current drilling motion of the user is similar to the skill

model. The result is used to adapt the value of variable stiffness gains in our learning-based control strategy (variable impedance control block) for producing guidance forces. In this approach, when a user moves the drill less similar to the reference skill model, greater guidance forces are applied to the end-effector and user's hand.

The dynamics of the robot is described by

$$f_H + f_{LbG} + f_{HR} = M\ddot{\boldsymbol{x}} + D\dot{\boldsymbol{x}} \tag{12}$$

where $\boldsymbol{x}$ is the position of the end-effector (drill bit), and M and D are positive-definite matrices representing inertia and damping, respectively. As shown in Fig. 7, the inputs to the robot are human applied force (f_H), haptic rendering force (f_{HR}), and additional virtual guidance force (f_{LbG}), which represents variable guidance force.

The users may feel two types of haptic force as follows. 1) Haptic force feedback produced to recreate sense of touch for the interaction between drill and the bone in virtual environment. 2) Guidance force that is only applied in practice mode for improving user performance. In the learning phase, for developing skill models (expert and resident models) the guidance force is set to zero to capture the real skill of users.

The inputs of the simulation system are patient specific CT data of femur bone and its segmentation. A semi-automatic segmentation method is used to separate the various layers of the bone: cortical bone, cancellous bone, and bone marrow. The

segmented bone data are used to build patient femur model by volume rendering. The density of voxels is assigned regarding to the intensity of pixels in the segmented CT data. The original CT matrix is also preserved for further X-ray simulation. The users are able to rotate the femur model with the mouse and take X-ray from any desired orientation. This results in simulating the actual process in the operation room.

The users interact with the model using a haptic device (Phantom Omni, Geomagic Touch, USA), a keyboard, and a computer mouse. Virtual drill can be manipulated to touch/drill the femur bone model through the stylus of the haptic device. In haptic rendering loop (1000 Hz), the current position and orientation of the haptic stylus are updated for calculating the transformation matrix of the drill as well as collision detection. If a collision between the drill and the bone is detected, force feedback are computed using the transformation matrix and the density of the intersected voxel. In the graphic rendering loop (30 Hz), the existence and intensity of a voxel is updated to generate the view of the bone volume model in the virtual environment (VE).

3.3 Learning-Based Guidance

This section presents the description of the learning-based approach that uses developed skill models to generate adaptive guidance forces and discriminate the skill levels of users. In the proposed approach, an HCRF-based skill model is developed

regarding the kinematic data of the expert motions associated with different bone layers. Adaptive guidance forces are generated in real time based on the similarity between the current motion of users and the skill model. Since bone layers have different stiffness, experts adjust drilling forces based on their experiences and skills to operate a smooth drilled path. Similarly, the guidance forces encourage users to follow the target path within the bone with less position error and more similar to the expert motions in terms of velocity, acceleration, and drilling temperature.

3.3.1   Learning-Based Skill Model

Since the analytical models of human motions/behavior are rarely available in HRI applications, the non-linear, non-stationary, and non-deterministic features of stochastic/statistical models make them powerful tools for modeling human behaviors, including the stochastic and uncertain human behavior in terms of both mental state and resulting actions [4, 23]. Stochastic modeling methods (i.e. HCRF) enable machine learning algorithms to 1) capture the spatial and temporal variation of the human motions, 2) capture the change in variance along the movement, and 3) tolerate noise and missing data.

In order to capture users' sequential dynamic characteristics and segment the drilling motion of a user within different bone layers, we develop an HCRF as a learning-based skill model for the training simulation. Generally the structure of hand motion sequences is complex and statistical models with hidden structures are powerful tools for recognition tasks, including human motion or gesture recognition

49

[41]. In addition, learning-based guidance (i.e. HCRF-based) has shown better user performance improvement, compared to constant haptic guidance [4]. HCRF models incorporate hidden state variables in a discriminative random field model to provide a way to determine a single label for an entire input sequence, e.g. the drilling motion of users. To model the motion of experts within bone layers, an HCRF model is developed by [41]:

$$P(y|O, \theta) = \sum_S P(y, S|O, \theta) = \frac{\sum_S e^{\psi(y, S, O; \theta)}}{\sum_{y' \in Y, S \in S^m} e^{\psi(y', S, O; \theta)}}, \tag{13}$$

where $y \in Y = \{Cortical\ bone,\ Cancellous\ Bone,\ Bone\ Marrow,\ Necrosis,\ None\}$ is the class label of the drill bit motion in and out of the bone, O is an observation sequence, S is the set of hidden states, and θ is the model parameters. $\psi(y, S, O; \theta)$, parametrized by θ, calculates the compatibility among a label, a set of observations and hidden states. In order to estimate the parameters, an objective function is utilized as follows [41]:

$$L(\theta) = \sum_{i=1}^{n} log P(y_i|o_i, \theta)) - \frac{1}{2\sigma^2} \|\theta\|^2, \tag{14}$$

where $\{y_i, o_i\}$ is the training set of labeled examples, n is the number of training sequence data, and σ^2 is the variance of a Gaussian prior. We use a Quasi-Newton optimization method, L-BFGS [54], for finding the optimal parameter values of trained HCRFs ($\theta^* = \arg \max_\theta\ L(\theta)$).

3.3.2 Adaptive Learning-Based Control

In real time, the proposed learning-based approach recognizes drilling motions and continuously generates motion similarity (MS) between the user motion and the trained HCRF:

$$MS(y, O_n) = \underset{y \in Y}{\arg \max} \; log \; P(y|O_n, \theta^*) \tag{15}$$

where O_n is the last n observation sequence of user motion.

$P(y|O_n, \theta^*)$ is a probability value that shows how much the current drill motion of the user is similar to the expert motion model. This HCRF-based similarity is used to determine the impedance control gain. An increase in the probability value leads to an increase in motion similarity.

An adaptive learning-based control scheme is used to lessen the effects of un-modeled dynamics, including unobserved deviations from a motion plan, and natural variability of human behavior. Guidance forces are calculated using the following equations:

$$f_{LbG} = -K_{LbG}(MS(y, O_n))[\boldsymbol{x} - \boldsymbol{x}_d] \tag{16}$$

where f_{LbG} is the guidance force, $K_{LbG} > 0$ is an adaptive stiffness gain depends on the motion similarity (MS) that is a typical probability function, $\boldsymbol{x}_d$ is the desired

position on the reference path, and $\boldsymbol{x}$ is the current position of the end-effector. The desired position, which is closest to x, is instantaneously found based on computational geometry methods [55].

The guidance force is computed using two terms: variable stiffness gain and the position error between the current end-effector position and the desired position. The direction of the guidance force is along with a line, joining the desired position and the current position.

A linear modulation function is selected for K_{LbG} to map each motion similarity value to the corresponding stiffness gain:

$$K_{LbG}(y, O_n) = \frac{K_{max} - K_{min}}{MS_{min} - MS_{max}}(MS(y, O_n) - MS_{max}) + K_{min} \tag{17}$$

where K_{min} and K_{max} are the maximum and minimum stiffness values. The values are selected in order for the safety of haptic device and giving users a good sense of the path they should follow, but they are able to stay outside the reference path, if necessary. MS_{min} and MS_{max}, which determine the range of MS, are selected based on the results of a pretest user study to minimize motion recognition error rate. This study also indicated that in the operation area of the system, the linear modulation is a fair mapping between MS and K_{LbG} to encourage residents drilling the bone more similar to experts. The stiffness gains are adaptively adjusted in real time according to the end-effector motions.

A windowing approach, in which the last short segments of real-time drill bit motion were sampled ($n = 5$ data points), was used to compute the motion similarity (MS) and guidance forces. Short window sizes may reduce the recognition accuracy of drill motions and accordingly the effectiveness of generated LbG forces. Long window sizes would result in latency and/or mistake in recognizing drill motions while the drill bit enters a bone layer from another one. The window size was experimentally selected to make a balance between these effects. Furthermore, a three-point moving average filter of previous stiffness gain data is used to smooth the stiffness gains and accordingly the guidance forces. The number of points is experimentally selected to obtain a smooth output signal.

According to passivity analysis, which is common for haptic simulations [56, 57], the coupling of the Phantom 1.0 haptic device and a VE is locally stable while the designated stiffness gains keep below 1015 N/m [56]. In this study, although using a different version of Phantom device, we selected a lower range of stiffness in the range 0-222 N/m, that was experimentally verified to lead to a stable haptic interaction.

3.4 Femur Bone Drilling Simulation

This section details the development of the simulation. First, we describe the creation of the bone model, which rendered based on patient-specific CT data (Section 3.4.1). Then, a voxel-based approach is developed to model the different stiffness of bone layers (Sections 3.4.2 and 3.4.3). To best of our knowledge, for the first time,

we use haptic interaction virtual forces generated in the virtual simulation for developing the skill models, evaluating users' skill, and producing guidance force in a kinesthetic learning-based approach. Next, we present our approach for generating user-defined X-ray views of the bone (Sections 3.4.5 and 3.4.6). Finally, the features of the developed graphical user interface are presented (Section 3.4.7).

3.4.1   Bone Modeling from CT Images

We use CT data of a patient suffering from femoral head necrosis to build a model for the simulation training system. Nowadays, CT and magnetic resonance imaging (MRI) are the two most common modalities that provide 3D medical images. MRI exceeds most in soft-tissue differentiation while CT, a tomography of X-ray by nature, is suited more for bone pathology diagnosis. Both bone density and strength information can be extracted from CT data [69]. We used a set of CT images of a femur bone as the basis of our visual and haptic modeling. The representative sample slices of different view angles and an initial rendering are shown in Fig. 8.
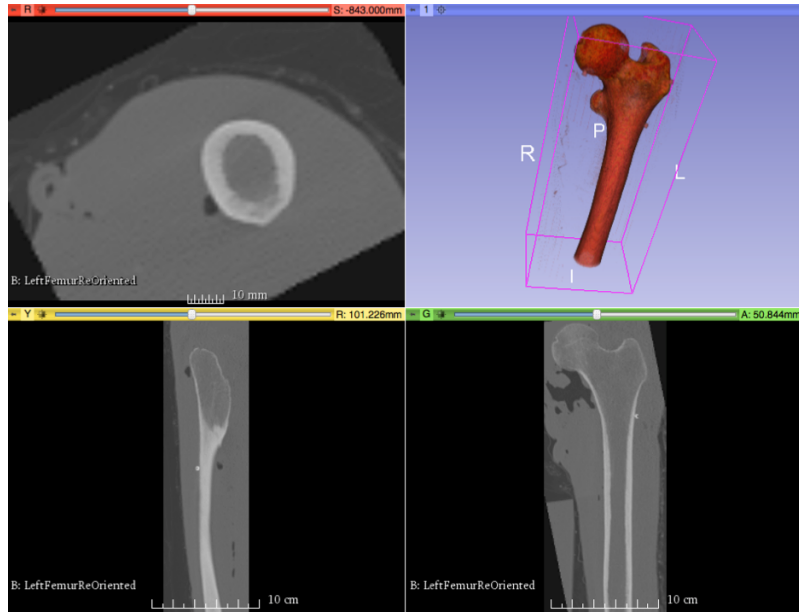
Figure 8: CT images as data source for modeling. Upper left: top view; Lower left: left view; Upper right: rendering display; Lower right: front view.

Intensity values on the CT images represent the attenuation coefficient of the tissue. The bright part in the slice is the cortical bone layer whose attenuation coefficient is high, and the dark parts are cancellous bone filled with bone marrow with low attenuations.

We segment the bone by developing a semi-automatic intensity-based thresholding method that requires several thresholds. Although an automatic thresholding method works well in the segmentation of the cortical layer, it often fails to differentiate the bone marrow part from the necrosis part in the femoral head, since in the latter case geometrical information also should be considered. This method includes thresholding; simple region growing algorithm using Robust Statistics Segmentation module in 3D Slicer. After careful adjustment and manual modification, cortical bone layer, femoral head necrosis, and bone marrow in the rest of the cavity are segmented apart

and turned into STL (STereoLithography) format surface models (see Fig. 9).
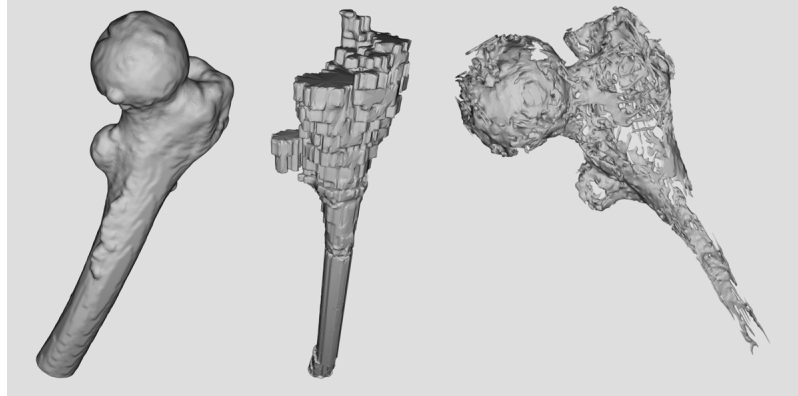
Figure 9: Surface models extracted from CT data. From left to right: Cortical bone surface, bone marrow, and necrosis.

3.4.2 Voxel-Based Rendering

We develop a volume rendering method with respect to bone drilling application and algorithm complexity. Since the tissue of interest is a hard bone, where drilling and tissue removal are the main operations, volume rendering has been preferred since it stores mechanical information at depth of the bone [70–73]. To address algorithm complexity, voxel removal is appropriately modeled in the method with respect to the fact that every voxel has its own density value. When the drilling force is applied on a set of voxels, their densities are reduced by a certain rate, and a voxel will be removed once its density becomes zero. Each voxel is associated with color, surface normal, and density information. The use of voxels also simplifies calculations while identifying interactions with the tool object.

A second rendering method is also developed to produce a more realistic model. To prepare the images for voxel rendering, the top view of the CT data is segmented

to distinguish the bone from the tissue, and remove the tissue from the images. The bone boundaries are identified with respect to the thresholds and filtered out small noise boundaries. Using a built-in colormap, the resulting model consists of voxels which their color values are based on the intensity values from the CT data. In addition, we use surface rendering for haptic display of the tool.

3.4.3 Stiffness Rendering

We consider the mechanical properties of bone layers for developing the simulation. The strength of cortical bone is usually larger than ten times of that of cancellous bone [74]. Brown et al. have studied mechanical property distributions, including stiffness and yield strength distributions, in femur region through direct mechanical measurements [75]. We use their results to adjust the stiffness of the bone layers.

The drilling speed and stiffness of voxel-based objects are completely dependent on the number of voxels that the drill bit is in contact with. However, using a large number of voxels to achieve low drilling speed could place a heavy burden on the graphic processor, as the voxel object would then be exponentially harder to render in the scene. To avoid this conflict, we utilize the color value of each voxel. First, since the application recognizes which voxel of an object is a part of upon contact, a transparency decrement is set for each object. The value is higher for high density bone and lower for low density bone. Upon contact, the transparency values are extracted from the contacted voxel and decremented by a fix value. Should the transparency value of a voxel reach zero, it is deleted from the scene. Second, the

intensity data from the CT scan are used to transfer the different intensity values of the pixels to the transparency values in each voxel. Similar to the first step, decreasing these values at various increments produces the same haptic feedback as drilling through different bone structures.

3.4.4 Drilling Motion

To further enhance the drilling experience, drill vibration is added to the simulation; whenever the drill bit point is in contact with the voxel object and the drilling button of the haptic device is pressed. Each bone layer has its own unique vibration amplitude and frequency. In regard to [73], we set these values so that material with higher stiffness would cause the drill to vibrate at a lower frequency and higher amplitude.

3.4.5 Virtual X-rays

One purpose of this study is to simulate the challenges of actual bone drilling operation. During the surgical treatment of osteonecrosis in OR, surgeons require to stop the drilling and change C-arm position for taking X-rays from different point of views. This assist them to ensure that the drill traverses the correct path within the bone. Our simulation is capable of illustrating the perspective 3D model of the bone as well as three X-ray views of the bone, including front, side, and top. As shown in Fig. 10, these features are simultaneously displayed to users.We use Euler angles to indicate the orientation of our field of view (FOV). The users can change projection direction during drilling. With these X-ray images overlaid with the real-time drill

projection, they can locate the 3D drill position, which is critical in actual surgeries.
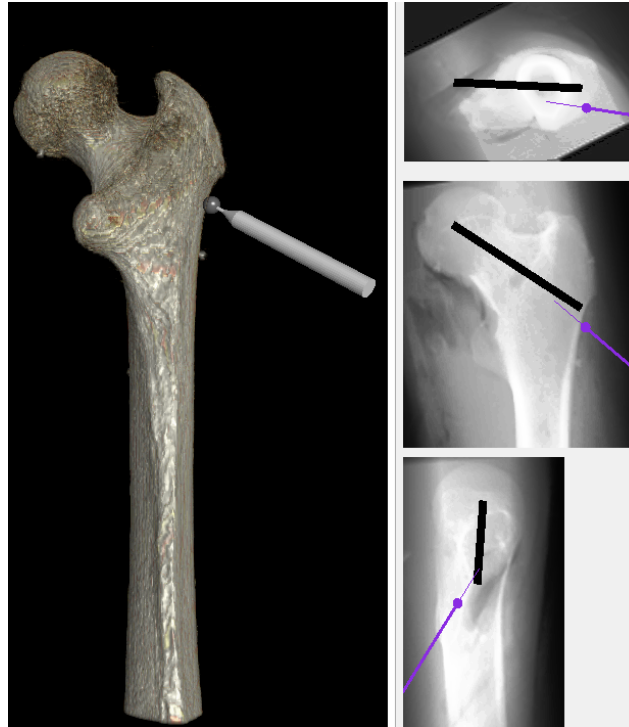
Figure 10: To easier perform the drilling task, users are provided with three X-ray views of the bone, the reference trajectory, and a line which shows the direction of the drill.

3.4.6 Mapping between CT Image and 3D Model

In order to show the right slice of the CT image when moving the plane in space, the relationship between 2D image and 3D model has to be determined. The mapping is based on the number of the slices and the size of the model. If the number of the CT images for front, side, top views are a, b, c ; and the size of the bounding box of the 3D model is $x \times y \times z$; the relationship is expressed as:

$$i = \frac{l}{a} \times x, j = \frac{m}{b} \times y, k = \frac{n}{c} \times z,$$

where i, j, k are the 3D coordinate in world frame correspond to the CT images and l, m, n are the index of the CT images.

3.4.7 Bone Temperature

The simulation also shows the current drill temperature. The bone temperature depends on drilling speed, drilling time or the applied force [76]. For the first time, to best of our knowledge, we simulate drilling bone temperatures, in which the temperature is generated regarding drilling parameters and the experimental data presented in the literature [76]. While the tissue is subject to temperatures more than $60°C$, bone tissue necrosis can be expected [77]. At lower temperatures, injury depends on the drilling time. The bone tissue can bear the temperatures of $45°C$ for more than 600s, $47°C$ for more than 60s and $50°C$ fo more than 30s to prevent thermal necrosis [76].

3.5 Experiment

The goal of this experiment is to investigate the efficacy of the learning-based approach in combination with the developed simulation to discriminate expert surgeons from novice residents and generate guidance forces in practice phase for improving

user performance.

3.5.1 Drill Motion Modeling

We train two HCRFs to model the five motions of drilling, the end-effector movement of experts/residents out of the bone (*None*) and within bone layers, including *Cortical Bone, Cancellous Bone, Bone Marrow,* and *Necrosis.* Although expert HCRF is used for generating guidance forces in addition to skill discrimination, resident HCRF is only used to discriminate the skill level of users.
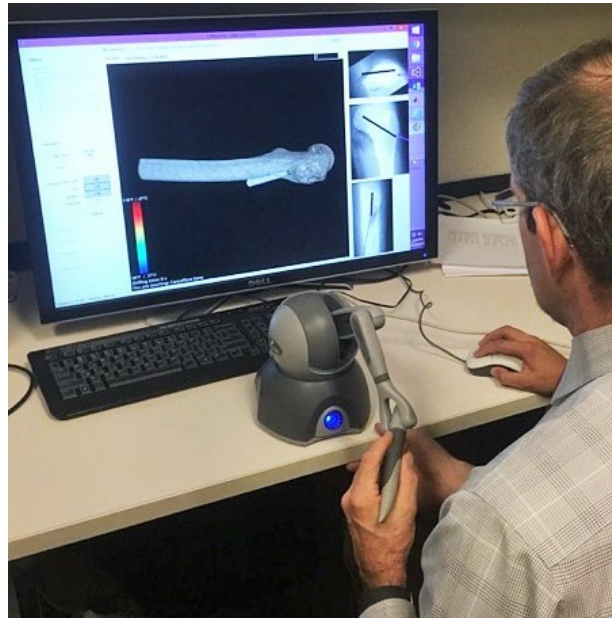
Figure 11: An expert surgeon while interacting with the simulation.

To train the expert HCRF, a data set was gathered from the demonstrations of five expert surgeons who interacted with the simulation through the haptic device and drilled the pre-planned path three times. Fig. 11 shows a surgeon while performing a demonstration. Seven surgical residents also demonstrated the task to

collect another data set for training the resident HCRF. Observed features included the position of the end-effector as well as the velocity and acceleration, which derived from the position. After the data collection, the data sets were segmented into the five class labels of the drilling motion. The expert and resident HCRFs were developed with 9 states and 12 states, respectively. The number of hidden states were set by minimizing the classification error rate on each training data set. The range of $[MS_{min}, MS_{max}] = [-2500, 0]$ and $[K_{min}, K_{max}] = [0, 250N/m]$ were selected for this experiment regarding the results of a pretest user study.

3.5.2 Procedure

Seven surgical residents (aged 28 to 33 with a mean age of 29.9 years) were asked to complete the task, which was drilling a pre-planed virtual path within the femur bone. We defined the pre-planned path, in which the residents had to pass through all the bone layers to get to the target point. A successful drilling task requires motor skills that improve task performance regarding creating a hole at the correct location without applying excessive force, over-penetration, heating, or skiving with the drill [78]. As shown in Fig. 10, during bone drilling, participants could see the three X-ray views of the bone, the reference trajectory (pre-planned path), and a thin line along the drill that shows the direction of the drill. The reference trajectory is a common drilling path in real surgery [79]. Every participant had five minutes to get familiar with the simulation and then carried out the task three times in the following LbG mode.

Learning-based Guidance (LbG): The developed expert HCRF model was used to provide adaptive stiffness gains and consequently generate guidance forces.

In the process of data collection for drill motion modeling, five experts and another seven residents had also performed the task, presented in Section 3.5.1, in the following mode.

No Guidance (NG): No guidance forces was provided to participants. The expert surgeons whose demonstrations are used to develop the expert HCRF are also the same who give the performance parameters of the task. The surgeons performed the task only in NG mode since they were experts in drilling and did not require guidance.

3.5.3   Results and Discussion

We use leave-one-out cross validation method to evaluate the skill discrimination performance of the trained models (expert and resident). We leave one trial of a drill motion out for testing and use the remaining trials for training the drill motion models. Since the collected datasets is not large enough, leave-one-out cross validation is selected for validation. Furthermore, this validation method has been used in the literature to calculate the recognition accuracy of surgical training sub-tasks [80] and residents' level of expertise [81]. The average of classification/recognition results for the two skil models (HCRFs) are presented in Table 5. The average percentage of expert motions that are correctly recognized by the expert model is 89.1%. This rate for the resident model is 88.4%. Considering the recognition of three motion labels

out of five for each drilling trial, the skill discrimination of a user as novice-level or expert-level results in 100% correct recognition. Taking into account of all the motion labels during a trial results in the increase of recognition rate to 100%, which is also observed in [24].

Table 5: Skill Recognition Rates (%) Based on Drill Motions

	Cortical	Cancellous	Marrow	Necrosis	None
Expert Model	87.1	86.3	94.9	83.6	93.6
Resident Model	86.1	92.8	89.5	79.6	94.0

To investigate the efficacy of the learning-based approach, we compare the performance of three groups: the five experts who performed the drilling task while no guidance is provided (E-NG), the seven residents who performed the task while LbG is provided (R-LbG), and the other seven residents with no guidance(R-NG). Three metrics are used to evaluate user performance: 1) the completion time of the bone drilling task, 2) the average root mean square error (RMSE) for the position error between the pre-planned path and the drilled path, and 3) the average variation of the bone temperature during the drilling task.

The means and standard errors (SE) of the completion time, position error, and average bone temperature across all participants are presented in Fig. 12. Table 6 shows the between-subject analysis of variance (ANOVA) results, with a rejection level of 0.05. The results of post-hoc Tukey-Kramer pairwise comparisons, $*$ ($P <$

0.05), are shown in Fig. 12. The results show that among the three groups, experts have significantly better performance in terms of completion time and average bone temperature. All the three performances for R-LbG are better than for R-NG. This indicates that providing the guidance forces improves the performance of residents.
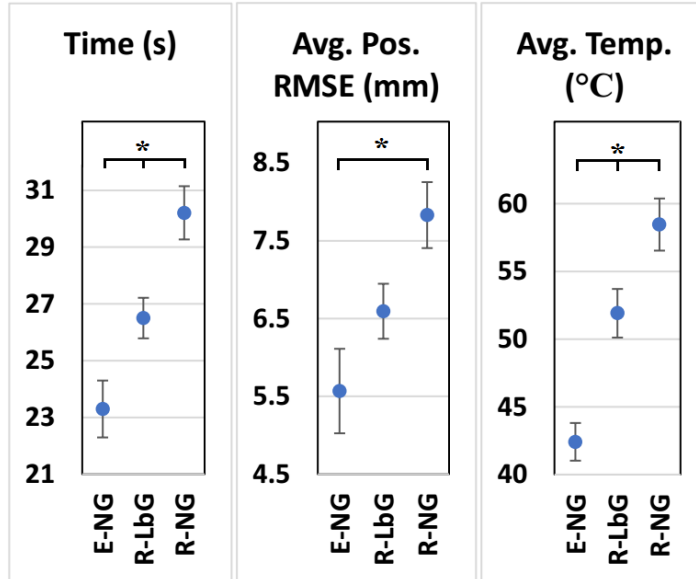
Figure 12: Means and standard errors of completion time, average RMSE for position, and average bone temperature across all participants for the three groups: experts with no guidance (E-NG), residents with the proposed guidance (R-LbG), and residents with no guidance (R-NG). The R-LbG group have significantly better time and average temperature compared to R-NG. * marks significant differences.

Table 6: ANOVA Results for the Performance Metrics. E-NG: experts with no guidance; R-LbG: residents with LbG; R-NG: residents with no guidance; SE: standard error

Metric	E-NG Mean(SE)	R-LbG Mean(SE)	R-NG Mean(SE)	$F(2,16)$	P-value
Time	23.29(1.00)	26.50(0.71)	30.21(0.98)	14.92	<0.001
RMSE	5.56(0.54)	6.59(0.35)	7.83(0.42)	6.5	0.003
Temp.	42.41(1.39)	51.91(1.79)	58.45(1.92)	24.35	<0.001

The results show that although our learning-based approach results in the improvement of resident performance, residents are not able to perform the task as skillful as the experts. The position error for the experts are not significantly better for R-LbG. The position error depend on the initial alignment of the drill in proper direction while a user starts drilling the bone. While the drill enters the bone, the user has less ability to maneuver the drill. The simulation provides the users with the three X-ray views of the bone to assist them in drilling with more appropriate alignment. This leads to lower RMSE.

Measuring the three metrics enables us not only to assess the skill of users objectively, but discriminate their skill level. The significant difference between the performance of experts and R-NG signifies that in addition to the HCRFs, the metrics can also be used to discriminate the skill level of users as experts or residents.

One idea behind this chapter is to investigate if we can manage to improve the

performance of the residents for a considered task using machine leaning-based guidance. To achieve this goal, we considered a femur drilling task and measured user performance for each method of providing force. The experiment has been conducted to investigate the performance of the two groups of residents. When force is applied, the performance of the residents significantly improves. However, as the force is not present, the second group of residents is not performing the task as well as the first group provided guidance forces.

One of the contributions of this work is to take the first step in investigating how machine learning-based guidance (LbG) could be used in surgery training by a clinical study. The focus of present work is mostly on studying *performance* not *learning effect*. Similarly, many researchers have been evaluated such learning-based (LfD-based) approaches only by investigating user/task performance [4, 7, 8].

3.6 Conclusion

This chapter presented a learning-based approach that aims to learn robots for transferring skills from expert to trainees. We developed the approach for both skill discrimination and user performance improvement in a virtual reality (VR) simulation for femur drilling surgery. Real CT data were used to provide the users with the feeling of bone stiffness variations in regard to the drilled depth. HCRF-based skill models (expert HCRF and resident HCRF) were developed from experts and residents demonstrations to segment the drill motion within different bone layers as well

as differentiate user's skill as experts or residents. In practice phase, the expert HCRF was used to adapt motion stiffness and generate learning-based guidance (LbG) for assisting residents with applying appropriate forces within different bone layers. A set of performance metrics was also used to objectively evaluate the skills of users.

The experimental results of our clinical study showed that LbG significantly improves residents performance in terms of completion time and average bone temperature. However, the residents were not able to perform a drilling task in a similar skill level of the experts. The results also indicated that in addition to skill models, performance metrics, including task completion time, RMSE for position, and average bone temperature, can be used to discriminate the skill levels of users.

In future work, the learning effects of the proposed LbG will be studied. In addition, a 6 DoF haptic devices will be used to provide more realistic virtual simulation.

Chapter 4

Towards Learning-Based Guidance for Skill Transfer in Human-Robot Teleoperation

This chapter presents a learning-based guidance (LbG) approach that assists operators to complete a task in teleoperated human-robot interactions. In this learning from demonstration (LfD) approach, teleoperation kinematic demonstrations in combination with kinesthetic demonstrations are used to develop a skill model. The temporal and spatial variation of demonstrations are learned using hidden Markov model (HMM) as the skill model. A modified Gaussian Mixture regression (GMR) in combination with the HMM is also developed to produce a continuous trajectory. The guidance forces are adaptively generated and provided to trainees based on similarities between trainee performance and the skill models in real time. This learning

based guidance encourages trainees to navigate a robot in a teleoperation system similar to the expert operators. In addition, we train two sets of skill models to investigate the effect of the incorporation of two variable impedance control methods into the LbG approach on the effectiveness of guidance forces. To experimentally evaluate our approach, a teleoperated robot is navigated through a haptic steering wheel and a haptic gas pedal. The results show that the performance of the users specially in terms of avoiding obstacles and task completion time is improved when guidance forces assist subjects.

4.1   Introduction

Human-robot interaction (HRI) is an extensive and diverse field of study [82]. One area of HRI applications is teleoperation in which humans perform manipulation and navigation tasks in remote environments to continuously control robot movements. Teleoperated robots enable humans to operate in hazardous or inaccessible environments. Another application area is automotive steering guidance that supports drivers with safety and driving subtasks, including lane keeping, lane changing, or obstacle avoidance [83–85].

The lack of time and skill of robot programmers may result in limited robot capabilities. Learning from demonstration (LfD) is a method for teaching robots that do not require the skill of expert programmers [3]. In this method, users demonstrate desired skills to a robot for performing new tasks, without any special knowledge

about the robot. A set of trajectories, which are the time-series sequences of teachers demonstration, is usually used to learn policies or skills for a task that may be generalized beyond the provided demonstrations. In robotics, it is a complicated procedure to explicitly plan a desired trajectory that meets task constraints as well as generalize movements in novel situations. During the reproduction phase of LfD, robots are able to optimize and generalize the movements onto similar motion in novel situations [86].

LfD enables robots to learn skills or motion behaviors from demonstrations in which the robots extract information from the demonstrations and develop learning-based models. Using these models, robots may assist humans to perform a collaborative task. Demonstrations can be provided through kinesthetic teaching and/or teleoperation [6–8, 68, 87]. In kinesthetic teaching, humans directly guide the robot's body to perform a task while in teleoperation human operates robots remotely and robot's sensors record the execution. LfD has widely been used for many robotic applications, including helicopter maneuvering [88], car parking [89], robot teleoperation [90], surgical training simulation [4], and robotic surgery [91].

Models of human operators (drivers) play an important role in systems that share control with operators (drivers) since human behavior is stochastic, unpredictable, and dependent on operation (driving) skills [85]. Using the natural response of drivers to traffic situations may results in better performance in a guidance-enabled driving system [92]. Furthermore, in unknown environments, robots face many challenges that humans are usually more adept in dealing with. As a result, robots assisting humans rather than replacing them in form of LfD has attracted many

researchers [23, 93–95]. The controllers can regulate the movements of the user for assisting and/or guiding purposes, depending on provided demonstrations and human skill models. They may apply force to guide the robot/human through a predefined sequence of motions, obstacle avoidance tasks, or to limit it [6, 14, 18, 29]. These control algorithms allow the robots to function in unstructured environments [96]. To control the interaction with unknown, unstructured and dynamically changing environments, impedance control proposed by Hogan [28] has been extensively used in HRI. Impedance control gains can be selected as constant values [18–20, 29, 30] or may adaptively be varied to assist users to perform dynamic tasks [4, 16, 31]. In the present work, each impedance control gain is adapted in real time based on a skill model that developed from a specific set of human/robot observations.

To model operator maneuvers, rather than using a time-dependent model of trajectories, the intrinsic dynamics of motions are considered using statistical models. Thus, the model is independent of explicit time variables and can generate trajectories with similar dynamics that were not covered during demonstration. Hidden Markov model (HMM) has been used as a statistical model that captures the spatial and temporal characterization of human/robot motions during demonstrations and reproduces human motions [97]. In addition, modified Gaussian Mixture regression (GMR) has been used in combination with HMM to robustly generalize the motion as the desired robot state to be achieved, in contrast to simple trajectories [6, 94, 98]. Similarly, we use HMM to learn a dynamic task as a sequence of action and modified GMR to produce reference robot states. However, we use HMM not only to learn and

recognize the dynamic model of demonstrated maneuvers of a teleoperation task, but also to generate adaptive guidance forces to steering wheel and gas pedal for avoiding collisions and performing smooth teleoperation maneuvers.

There has also been many research on haptic enabled teleoperations. A major application of mobile robot teleoperation is to explore remote areas like battle fields or hazardous chemical regions [99]. The robot-obstacle distance for computing the feedback forces has been used in previous work, where a designated haptic manipulator probe is used to impart the translational velocity and angular velocity to the robot. The results have suggested that haptic has a significant effect in reducing the number of collisions, and to decrease the minimum robot-obstacle distance [99–103].

Haptic-enabled systems have also been used to support humans in driving tasks, including car following [92], navigation [104], and eco-driving [105]. Haptic can be provided to drivers through steering wheel, gas pedal, seat, or seat belt. An important objective of the haptic systems is to avoid collisions, evade stationary obstacles, or pedestrians [104, 106, 107]. Mulder et al. have proposed a few haptic algorithms for haptic gas pedal feedback for active car-following support [92,106]. Farkhatdinov et al. [104] have proposed a force feedback rendering strategy for mobile robot teleoperation with variable feedback gain, where gain is a function of the robot-obstacle distance and the derivatives of it. They modify the stiffness of a linear impedance control strategy [28] based on the distance to the obstacle and its derivative. Their results suggest that this approach reduces the magnitude of the force provided to the teleoperator and improves the accuracy of the operation. In the present chapter, we propose the

addition of an LfD method as well as the geometrical distance and velocity relative to obstacles in order to adjust the adaptive stiffness and damping gains of impedance control.

In this work, we develop a learning-based guidance approach that can provide operators with guidance forces to improve safety, keep lane, and avoid obstacle collision. The forces are delivered on the steering wheel and gas pedal that augment to the usual force feedback of steering and pedal systems. We use the demonstrations of expert operators while performing a teleoperation task to capture their navigation skills. Robot motions are learned from the demonstrations using an HMM, and a modified GMR is developed to use implicit temporal information from the statistical model, HMM, for generating continuous reference motion during reproduction phase. In real time, the skill model adapts the gains of several variable impedance controllers. In addition, the distance between the robot and obstacles is incorporated into the impedance control to generate guidance forces that also assist operators with avoiding obstacle collisions. For the evaluation and implementation of our approach, a haptic enabled setup is developed which the guidance forces are provided to a teleoperated robot through a gas pedal and a steering wheel.

A main contribution of this chapter is to develop skill models using a combination of both kinesthetic teaching demonstrations (kinesthetic of pedal and steering) as well as teleoperation demonstrations (kinematic of the teleoperator). Each skill model is used a distinct kinematic dataset to learn a specific teleoperating skill regarding the characteristics of that skill. In addition, LfD-based skill models are

incorporated into single-gain variable impedance control (SV-VIC) and multiple-gain variable impedance control (MV-VIC). The capabilities of these two impedance control methods for generating LbG forces are compared in terms of the performance of teleoperation. Finally, to our best knowledge, for the first time in this chapter, a learning-based approach is developed for the adaptive guidance of a teleoperator through both *haptic steering wheel* and *haptic gas pedal.*

The outline of this chapter comprises as follows. In Section 4.2, the learning-based guidance and the model of the system is discussed in details. Section 4.3, presents the experimental studies to evaluate the effectiveness of the proposed approach. In Section 4.4, the conclusions and future work are presented.

4.2   Learning-Based Guidance

This section presents the description of the learning-based approach that uses developed skill models to generate adaptive guidance forces.

4.2.1   General Architecture

In the proposed approach, HMM-based skill models are developed regarding the demonstration of expert operators in which they follow a target path without any collisions. A combination of HMM with GMR is used to generate continuous reference paths from the demonstrations [98]. Adaptive guidance forces are generated in real time based on the similarity between the current maneuver of users and the

skill model. To avoid collision, experts smoothly adjust the direction and velocity of the robot based on their experiences and skills. During reproduction, the guidance forces encourage users to follow the reference path with less obstacle collisions and less completion time. In this work, we use adaptive guidance forces for teleoperator navigation since learning-based guidance (i.e. HMM-based) has shown better user performance improvement, compared to constant haptic guidance [4].

Fig. 13 describes the block diagram representation of the LbG approach. Our framework consists of a haptic steering wheel and haptic gas pedal, a wireless network, and a teleoperated robot (DaNI robot). The input forces from the human (user's) hands and foot are represented as f_{s-h} and f_{p-h}. These forces manipulate the direction of movement through steering wheel angle θ_s and the velocity of the robot through pedal angle θ_p. Applying LbG forces (f_{s-LbG} and f_{p-LbG}), when a user moves the steering/pedal less similar to the skill models, more guidance forces are applied to steering/pedal (the hands/foot of the user) to encourage the user to perform correct maneuvers.

The robot continuously interacts with the environment and the resulting data is collected within its sensing range. In this work, the ultra sonic sensor mounted on the robot gathers the distance (d) and angle (ϕ) to the obstacle within its range. The data is communicated to the robot through a wireless network. The network is local and the issue of latency can be disregarded.
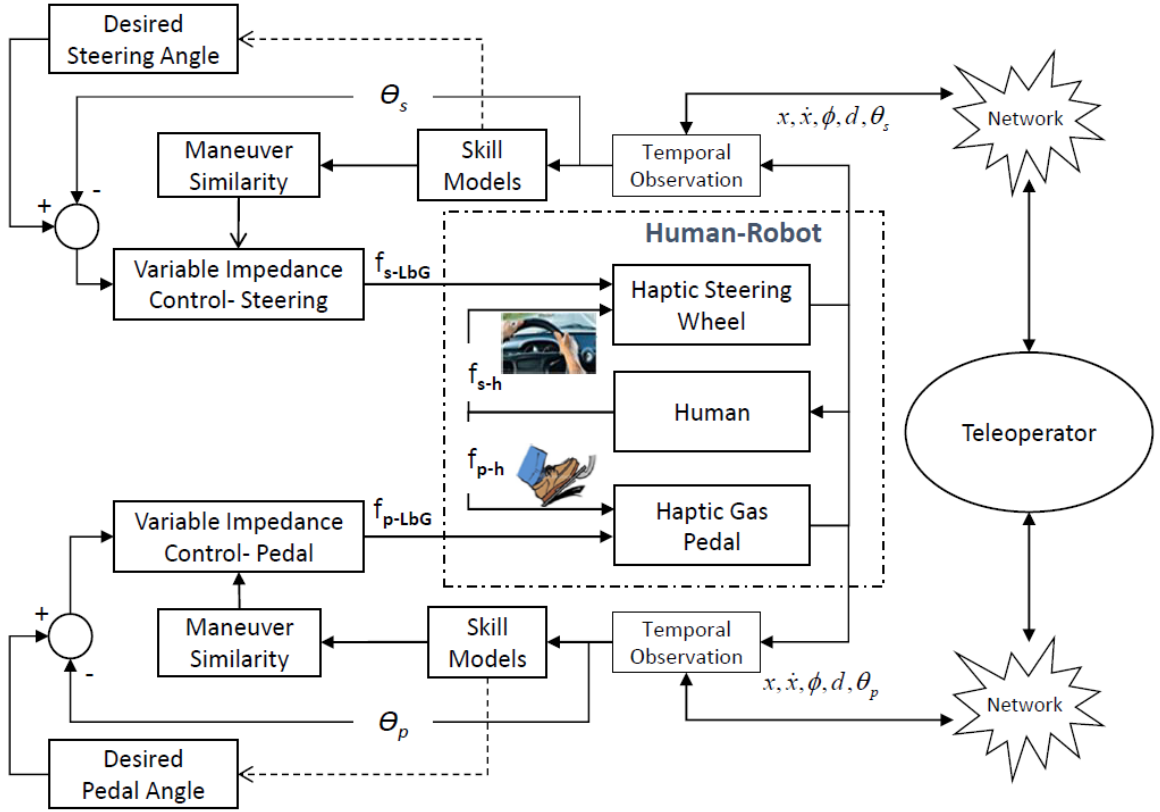
Figure 13: The block diagram representation of the learning-based guidance (LbG) approach. The human input forces to the system (f_{s-h} and f_{p-h}) and calculated LbG forces from the system to the human (f_{s-LbG} and f_{p-LbG}) are applied through the steering wheel and gas pedal. An expert skill models is used to generate maneuver similarity and resulting adaptive impedance gains based on the similarities between current angular motion of steering (θ_s)/pedal (θ_p) and the reference skill model. A variable impedance control strategy calculates forces to guide the user for following desired angles. The distance (d) and angle (ϕ) to the obstacle are also incorporated into the impedance control to avoid collision with obstacles. Temporal observations are angle of steering wheel, angle of gas pedal, as well as the position and velocity of the teleoperator.

4.2.2 Learning and Generation of Motions

The examples of successful teleoperation demonstrations are used to learn the robot. To capture the sequential dynamic properties of robot motions, we develop continuous HMMs with Gaussian mixture distribution for a teleoperation task. A K-state

$\{S_1, S_2, ..., S_K\}$ continuous HMM with a Gaussian observation, $\lambda = (A, B, \pi)$, is defined by three parameters [53]: a state transition probability distribution $A = \{a_{ij}\} = P(S_t = j \mid S_{t-1} = i)$, a set of observation model probabilities $B = P(O_t|S_t)$, and a set of prior probabilities $\pi = \pi_i$, where $\pi_i = P(S_1 = i)$ and $1 \leq i, j \leq K$.

Since the actual observation sequence is continuous, generating a continuous output requires estimating the probability density function (pdf) of the state output (observation model). To model this density, the set of demonstrations is used to estimate the Gaussian mixture parameters. The M-mixture of observation model is defined as follows.

$$P(O_t = o|S_t = i) = \sum_{m=1}^{M} P(M_t = m|S_t = i)\mathcal{N}(o; \mu_{m,i}, \Sigma_{m,i}) \tag{18}$$

where $\mathcal{N}(o; \mu, \Sigma)$ is the Gaussian density, μ_i and Σ_i are the mean and covariance of the state i, O_t is the observation, S_t is the state, M_t is a hidden variable that specifies which mixture component to use, and $P(M_t = m|S_t = i) = c(i, m)$ is the conditional coefficient of each mixture component. The input and output of each state can be represented by

$$\mu_i = \begin{bmatrix} \mu_i^\theta \\ \mu_i^{\dot{\theta}} \end{bmatrix} \; and \; \Sigma_i = \begin{bmatrix} \Sigma_i^\theta & \Sigma_i^{\theta\dot{\theta}} \\ \Sigma_i^{\dot{\theta}\theta} & \Sigma_i^{\dot{\theta}} \end{bmatrix}, \tag{19}$$

where θ and $\dot{\theta}$ are the angular position and velocity of the steering/pedal, respectively.

In order for generating the reference trajectory and avoiding time scaling, joint distributions are learned and conditional probabilities are used. To achieve this, the covariance between the position and velocity is learned using the HMM. We employ GMR and calculate a likelihood using the HMM representation to capture temporal and spatial data probabilistically encapsulated in the HMM. In other words, the original GMR weights are replaced with their HMM's counterpart as follows [98]:

$$h_i(o_t) = \frac{\alpha_{i,t}}{\sum_{k=1}^{K} \alpha_{k,t}} \tag{20}$$

$$\alpha_{i,t} = \left(\sum_{k=1}^{K} \alpha_{k,t-1} a_{ki}\right) \mathcal{N}(o_t; \mu_i^\theta, \Sigma_i^\theta),$$

where h_i is the weight factor that is modified HMM *forward* variable and $\alpha_{i,t}$ is the probability of being in state i at time t for the sequence of given observation $O_t = \{o_1, o_2, ..., , o_t\}$ [53].

In real-time reproduction, the desired angular position and velocity trajectories are estimated through the GMR at each time step [98]:

$$\hat{\theta} = \sum_{k=1}^{K} h_i(o_t)[\mu_i^\theta + \Sigma_i^{\theta\dot{\theta}}(\Sigma_i^{\dot{\theta}})^{-1}(\dot{\theta} - \mu_i^{\dot{\theta}})] \; and \tag{21}$$

$$\hat{\theta} = \sum_{k=1}^{K} h_i(o_t)[\mu_i^{\dot{\theta}} + \Sigma_i^{\dot{\theta}\theta}(\Sigma_i^{\theta})^{-1}(\theta - \mu_i^{\theta})].$$ (22)

4.2.3   Variable Learning-Based Impedance Control

In reproduction phase, the proposed learning-based approach continuously generates maneuver similarity (MS) between the user motion and the learned skill models, HMMs:

$$MS_l(y, O_n) = \arg \max_{y \in Y} \ log \ P(O_n, |\lambda_l)$$ (23)

where O_n is the last n observation sequence of user motion and λ_l ($l \in \{K, B\}$) are skill models (HMMs) that adapt the stiffness and damping gains of impedance control. The features of each skill model is chosen regarding the steering motion, pedal motion as well as the position and velocity of the teleoperator. The details of skill model training are presented in Section 4.3.1.

$P(O_n, |\lambda_l)$ is a probability value that shows how much the current pedal/steering maneuver of a user is similar to the expert skill models. This HMM-based similarity is used to determine the impedance control gain. An increase in the probability value leads to an increase in maneuver similarity.

A variable learning-based control scheme is used to lessen the effects of unmodeled

dynamics, including unobserved deviations from a motion plan, and natural variabil-
ity of human behavior. Generally, LbG forces are calculated using the following
equations:

$$f_{LbG} = -K_{LbG}(y, O_n)[\theta - \hat{\theta}] - B_{LbG}(y, O_n)[\dot{\theta} - \dot{\hat{\theta}}] \qquad (24)$$

where f_{LbG} is the guidance force, $K_{LbG}(y, O_n) > 0$ and $B_{LbG}(y, O_n) > 0$ are adap-
tive stiffness and damping gains depend on the maneuver similarity (MS) that is a
typical probability function. $\hat{\theta}$ is the desired angular position on the desired angular
trajectory, and θ is the current angular position of the steering/pedal.

The skill models are developed such that the variable impedance control follows
the subspace position and velocity of the demonstration of expert operators. λ_K
and λ_B are used to adjust learning-based stiffness (K_{LbG}) and and learning-based
damping (B_{LbG}) gains, respectively. An HMM can be considered as a particular form
of finite state machine in which transitions between states are probabilistic rather
than deterministic (see Fig. 14). Therefore, control gains (K_{LbG} and B_{LbG}) are
continuously adapted regarding finite state machines (skill models) in real time.
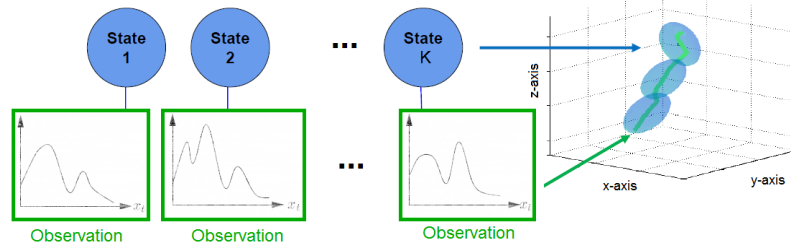
Figure 14: A schematic of a K-state hidden Markov model (HMM) that can be considered as a form of finite state machine for encoding steering/pedal motions.

In addition, we develop two impedance control methods to generate LbG forces. In the first method, guidance forces are computed based on the adaption of a single control gain (described in Section 4.2.6). In the second method, two control gains are simultaneously adapted to generate guidance forces (presented in Section 4.2.7).

Linear modulation functions are selected for K_{LbG} and B_{LbG} to map each maneuver similarity value to the corresponding impedance control gain:

$$K_{LbG}(y, O_n) = \frac{K_{max} - K_{min}}{MS_{min} - MS_{max}}(MS_K(y, O_n) - MS_{max}) + K_{min} \qquad (25)$$

$$B_{LbG}(y, O_n) = \frac{B_{max} - B_{min}}{MS_{min} - MS_{max}}(MS_B(y, O_n) - MS_{max}) + B_{min} \qquad (26)$$

where $K_{min} \leq K_{LbG} \leq K_{max}$, $B_{min} \leq B_{LbG} \leq B_{max}$, and $MS_{min} \leq MS_{K/B} \leq MS_{max}$. K_{min}/B_{min} and K_{max}/B_{max} are the maximum and minimum stiffness/-damping values. The values are selected in order for the safety of steering/pedal and

82

giving users a good sense of the path they should follow, but they are able to stay outside the reference path, if necessary. MS_{min} and MS_{max}, which determine the range of MS, are selected based on the results of a pretest user study to minimize motion recognition error rate. This pretest study also indicated that in the operation area of the system, the linear modulation is a fair mapping between MS and K_{LbG}/B_{LbG} to encourage users to navigate more similar to expert operators. The stiffness gains are adaptively adjusted in real time according to the steering/pedal motions.

In real time, a 0.10s sliding window with step size 0.02s is used for updating control gains and LbG forces. We restrict the time windows to only use data from the past to avoid any latency. A five-point moving average filter of previous stiffness gain data is used to smooth the stiffness gains and accordingly the guidance forces. The number of points is experimentally selected to obtain a smooth output signal.

4.2.4 Dynamic Model of Gas Pedal

This subsection presents the model of pedals motion. In order to represent the torque acting on the pivot point in terms of force, the distance between the pivot point and the perpendicular line to the foot, D_{ppf}, is calculated as:

$$D_{ppf} = \frac{\cos{(\psi)}}{\sqrt{{d_1}^2 + {d_3}^2}} \tag{27}$$
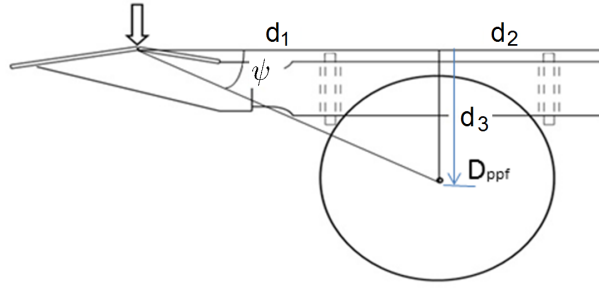
Figure 15: Representation of the input force of the user on the gas pedal.

Using (27), the relation between torque at the pivot point and the force is obtained by:

$$T_p = D_{ppf}(f_{p-h} + f_{p-LbG}) \tag{28}$$

where T_p is the torque acting on the pedal and F_{p-h} is the user's input force on the gas pedal.

The equation for the torque acting on the pedal is given by:

$$T_p = I_g\ddot{\theta}_p + \Gamma_g\dot{\theta}_p + K_p\theta_p \tag{29}$$

where I_g is the moment of inertia of the pedal, Γ_g is the rotational damping of the gas pedal, K_p is the linear spring constant, and θ_p is the angular displacement of the pedal.

Similarly for the steering wheel, the mathematical formulations could be represented as:

$$T_s = d_c(f_{s-h} + f_{s-LbG}) \tag{30}$$

where T_s is the torque at the steering wheel, d_c is the distance from the center to the edge of the steering wheel, and f_s is the tangential force on the steering wheel.

The torque acting on the steering wheel could be calculated using:

$$T_s = I_s\ddot{\theta}_s + \Gamma_s\dot{\theta}_s + K_s\theta_s \tag{31}$$

where, θ_s is the angle of the steering wheel, I_s is the moment of inertia for the steering wheel, and Γ_s is the rotational damping of the steering wheel. This model was validated using a force transducer that was designed for automotive uses.

4.2.5 Teleoperator Model

The DaNI robot from National Instruments as a skid-steered robot (teleoperator) is used in this study to implement and evaluate the proposed LbG approach. In skid-steered robots, the orientation of the robot is controlled by applying the same torque on the wheels of the same side and a different torque on the other side. To mathematically describe the dynamics of skid-steered robots, we consider the teleoperated robot moving at a constant velocity about an instantaneous center of rotation

as shown in Fig. 16 [1].

The global and local coordinate frames are denoted by X-Y and x-y, respectively. The variables v, $\dot{\phi}$, and R are translational velocity, angular velocity, and turning radius of the robot, respectively. As shown in Fig. 16, the robot is a four-wheeled skid steered robot, so ICR_l and ICR_r respectively represent the instantaneous center of rotation for left and right wheels of the robot.
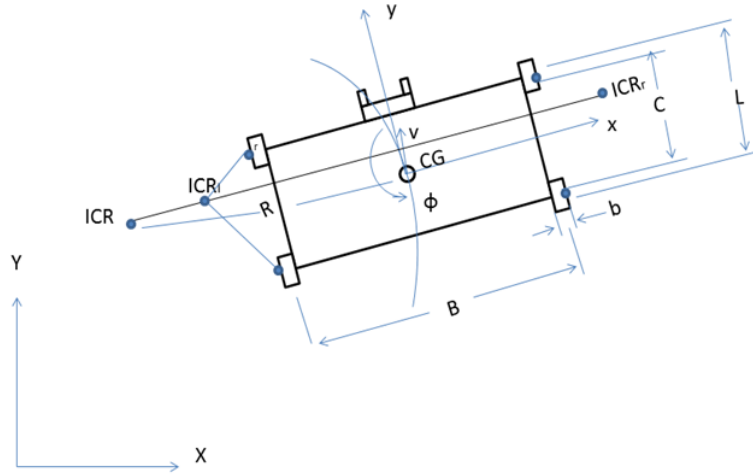
Figure 16: The kinematics of a skid-steered robot and the corresponding instantaneous center of rotation [1].

In the x-y frame (local co-ordinates), the coordinates of ICR, ICR_l and ICR_r are described as (x_{ICR}, y_{ICR}), (x_{ICRl}, y_{ICRl}), and (x_{ICRr}, y_{ICRr}), respectively. The robot's velocity is denoted as $u = [v_x \ v_y \ \dot{\phi}]^T$, where v_x, v_y are components of the velocity along x and y axes. The angular velocities of the left wheel is represented by ω_l, and for the right wheel is denoted by ω_r. The parameters b, B, and r are wheel's width, robot's width, and wheel's radius, respectively.

86

The experimental kinematic model of a skid-steered wheeled robot is given by:

$$
\begin{bmatrix} v_x \\ v_y \\ \dot{\phi} \end{bmatrix} = \frac{r}{x_{ICRr} - x_{ICRl}} \begin{bmatrix} -y_{ICR} & y_{ICR} \\ x_{ICRr} & -x_{ICRl} \\ -1 & 1 \end{bmatrix} \begin{bmatrix} \omega_l \\ \omega_r \end{bmatrix} \tag{32}
$$

Since skid-steered robot is symmetric about x and y axes, then $y_{ICRl} = y_{ICRr} = 0$ and $x_{ICRl} = -x_{ICRr}$. Expansion factor α is defined as the ratio of the longitudinal distance between the left and right wheels over the robot's width and could be presented as:

$$
\alpha \cong \frac{x_{ICRr} - x_{ICRl}}{B} \tag{33}
$$

As a result, for a symmetric robot the kinematic model in (32) is represented as:

$$
\begin{bmatrix} v_y \\ \dot{\phi} \end{bmatrix} = \frac{r}{\alpha B} \begin{bmatrix} \frac{\alpha B}{2} & \frac{\alpha B}{2} \\ -1 & 1 \end{bmatrix} \begin{bmatrix} \omega_l \\ \omega_r \end{bmatrix} \tag{34}
$$

4.2.6 Single-Gain Variable Impedance Control (SG-VIC)

In this method, only a single gain of the impedance controller is adapted in real time with regard to variable stiffness gain (K_{LbG}) and geometrical obstacle force.

The dynamic obstacle force on the steering is based on the assumption of having a virtual spring between the robot and the obstacle. The spring is positioned along the horizontal component of the distance vector. This representation is shown in Fig. 17.
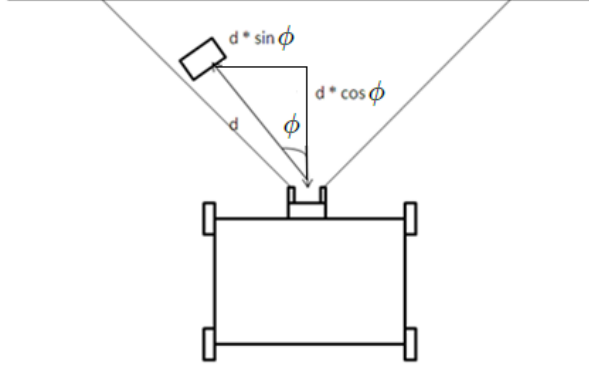
Figure 17: Geometry of dynamic obstacle force for collision avoidance. The obstacle force on steering is a function of the horizontal component of the distance to the obstacle. The obstacle force on gas pedal depends on the vertical component of the velocity relative to the obstacle.

Considering (24) and (25), we define a geometry-based guidance force on the steering wheel as:

$$f_{s-LbG} = -\frac{K_{LbG}}{d\ sin(\phi)}(\theta_s - \hat{\theta}_s) \tag{35}$$

where $0 \leq \phi < \frac{\pi}{2}$ and stiffness, K_{LbG} is learning-based stiffness gain, $\hat{\theta}_s$ is the desired steering angle calculated using (21), and $dsin(\phi)$ is the horizontal component of the distance to the obstacle. Using this equation, the magnitude of the stiffness gain decreases with the distance to the obstacle. Thus, repellent guidance forces are stronger if the robot approaches the obstacle head on. In addition, there is a less

chance for false guidance force when the user intends to just pass by an obstacle. In order to calculate the maneuver similarity between the current operator maneuvers and the stiffness skill model (λ_K), we use the current observations of the steering, pedal and teleoperator, including steering angle, steering velocity, pedal angle, pedal velocity, distance to the obstacle, angle to the obstacle as well as the position of the teleoperator.

For gas pedal, the LbG force using a spring model is described similar to (35), as:

$$f_{p-LbG} = -K_{LbG} \, \|v\| \, cos(\phi) \, (\theta_p - \hat{\theta}_p) \tag{36}$$

where $0 \leq \phi < \frac{\pi}{2}$, $\hat{\theta}_p$ is the desired gas pedal angle calculated using (21), v is velocity relative to the obstacle, and $\|v\| cos(\phi)$ is the vertical component of the velocity. Using this LbG approach, the magnitude of the stiffness gain and resulting guidance force increases with the relative velocity and is zero when $\|v\|$ is zero.

The next subsection describes another method, in which two learning-based gains of impedance controller are adaptive.

4.2.7 Multiple-Gain Variable Impedance Control (MG-VIC)

In this method, two gains of the impedance controller is adapted in real time with regard to learning-based stiffness gain (K_{LbG}), learning-based damping gain (B_{LbG}), and geometrical obstacle force. Similar to SG-VIC method, the horizontal component

89

of the distance corresponds to the steering wheel and the vertical component of the distance corresponds to the gas pedal.

In this method, the damping impedance gain is varied based on a skill model that captured the velocity of the teleoperator, the steering, and the pedal. The current observations of the steering, pedal and teleoperator, including steering angle, steering velocity, pedal angle, pedal velocity, distance to the obstacle, angle to the obstacle as well as the velocity of the teleoperator, are used to calculate the maneuver similarity between the current operator maneuvers and the damping skill model (λ_B). In this scenario, the conjunction of the damper with the spring is to render smoother forces and improve the control of the robot.

Using (24), (26) the guidance force on steering is defined as:

$$f_{s-LbG} = -\frac{K_{LbG}}{d\ sin(\phi)}(\theta_s - \hat{\theta}_s) - \frac{B_{LbG}}{d\ sin(\phi)}(\dot{\theta}_s - \hat{\dot{\theta}}_s)\ , \tag{37}$$

where $\hat{\dot{\theta}}_s$ is the desired angular velocity of the steering computed by (22).

Similarly, the equation for the guidance force on the gas pedal is:

$$f_{p-LbG} = -K_{LbG}\ \|v\|\ cos(\phi)(\theta_p - \hat{\theta}_p) - B_{LbG}\ \|v\|\ cos(\phi)(\dot{\theta}_p - \hat{\dot{\theta}}_p), \tag{38}$$

where $\hat{\dot{\theta}}_p$ is the desired angular velocity of the gas pedal calculated by (22).

4.3 Evaluation

In this section, the implementation of proposed methods for generating the guidance forces described in Section 4.2 and their experimental evaluation are presented.

4.3.1 Learning Skill Models

Three HMM-based skill models are trained to capture the skill of expert operators and consequently generate impedance control gains. The models include λ_K and λ_B that adjust the stiffness and damping gains, respectively. Each skill model uses a set of related observations/features to adapt corresponding control gain. The common observations are steering angle, steering velocity, pedal angle, pedal velocity, distance to the obstacle, angle to the obstacle, which used for training all skill models. In addition, the position and velocity of the teleoperated robot are added to the observation of λ_K and λ_B, respectively. Two other HMMs (λ_{θ_s}, λ_{θ_p}) are also developed to learn the motions of steering/pedal (θ_s/θ_p) from demonstrations and to retrieve a generalized form of trajectories. These two models are trained using the position and velocity of steering/pedal for generating desired trajectories as described in Section 4.2.2.

To develop the skill models, a data set was collected from eleven users' demonstrations. The users had two hours to practice with the setup and then performed a predefined teleoperation task three times, while no guidance is provided. The users can be considered experts in performing maneuverings, compared with new users.

Successful demonstrations with smooth robot motion and no collision were selected as observations to train the models. Bakis (left-to-right) topology [53] was used for developing the HMMs because this topology efficiently describes the sequential nature of motions. The HMMs were developed with 25 states, a mixture of two continuous Gaussian probability distributions, and the average recognition/classification accuracy of 85.2%.

The number of hidden states in HMMs were set by Bayesian Information Criterion (BIC) [108] algorithm. A windowing approach, in which short segments of real-time steering/pedal motion were sampled ($n = 5$ data points), was used to compute the maneuver similarity (MS) and LbG forces.

To learn generalized models of the kinematics and kinesthetic of a teleoperation task, we model motions as a nonlinear Dynamical System (DS). The DS is modeled by HMM and GMR; trained with the Stable Estimator of Dynamical Systems (SEDS) [108] algorithm to guarantee that the system is stable and the motions converge to desired steering/pedal angle regardless of starting position. Using SEDS, we can ensure that the motions follow closely the expert demonstrations.

4.3.2 Procedure

Fig. 18 shows a participant who interacts with our experimental setup. The teleoperated robot, DaNI robot, is connected to the wireless network through the travel router mounted on it. The robot is controlled wirelessly from the remote computer. The physical motion of the robot is controlled by a Logitech Driving Force Feedback

GT steering wheel and a haptic pedal.
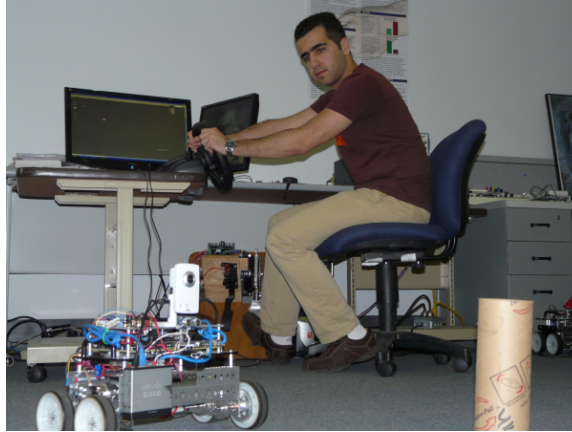
Figure 18: A participant while navigating the teleoperated robot using the steering wheel and the gas pedal.

Twenty participants (aged 18 to 23 with a mean age of 20.9 years) participated in this study. The participants were asked to run the robot with the steering wheel and gas pedal for ten minutes to get familiar with use of the setup. All participants were made aware of the parameters that are monitored during the experiment. They were to maneuver the robot in a random track and to perform a task with minimum number of collisions with obstacles. Fig. 19 demonstrates a track.

Using both steering wheel and gas pedal, the discussed impedance control methods in Section 4.2 are evaluated. The steering wheel was used for controlling the orientation of the robot, however, the gas pedal was used to control the forward motion of the robot. Every subject performed the task in the following three modes:
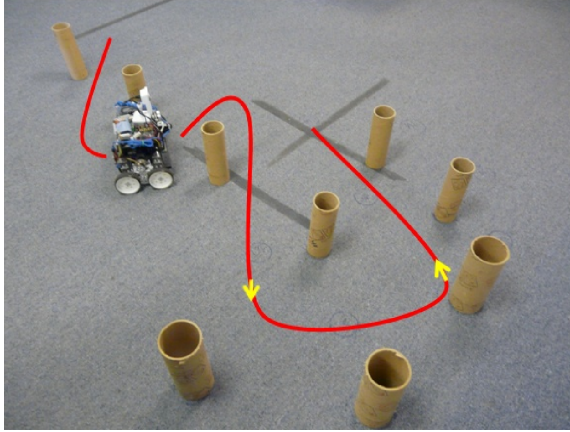
Figure 19: A track in which the robot is moving.

1. **No Guidance**: the participants performed the task with no guidance forces on steering wheel or on the gas pedal.

2. **SG-VIC**: during the experiment, LbG force is rendered on the steering wheel and gas pedal based on (35) and (36). Only a single control gain of the impedance control (K_{LbG}) is adjusted in real time.

3. **MG-VIC**: For this mode, the magnitude of the LbG force is governed by (37) and (38). Two control gains of the impedance control (K_{LbG} and B_{LbG}) are adapted in real time to encourage the users to perform the task similar to expert operator demonstrations.

4.3.3 Results and Discussion

The means and standard errors across all participants are shown in Figs. 20, 21, and 22 for the three modes: No Guidance, Single-Gain Variable Impedance Control (SG-VIC), and Multiple-Gain Variable Impedance Control (MG-VIC). Table 7 shows

the ANOVA results of this experiment. There are statistically significant differences for the three metrics among the three modes. Thus, Bonferroni post-hoc analysis is conducted to examine statistically differences between pairwise measured performance metrics. In Figs. 20, 21, and 22, * indicates significant differences with $P < 0.05$.

Fig. 20 shows the comparison of the average number of collisions across all the methods discussed. The figure suggests that the MG-VIC method has a distinct advantage over the other methods in terms of decreasing the average number of collisions. The results also confirm that providing LbG forces (SG-VIC and MG-VIC) has significantly improved the performance of users. Similarly, Brandt et al. [107] have shown a decrease in collisions when a haptic system used a combination of a lane-keeping and a collision-avoidance assistance system.
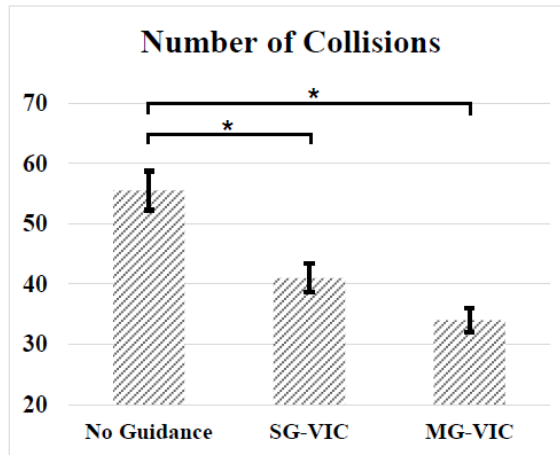
Figure 20: Graph representing the average number of collisions with standard error for the considered methods. The results confirm that proving the LbG forces improves the performance. Furthermore, it seems that the MG-VIC method is more effective than other methods. * shows significant differences with $P < 0.05$.

Fig. 21 represents the average time of completion in seconds. Completion time for MG-VIC is significantly better than for No Guidance. While for completion time,

the Bonferroni post-hoc test found no significant differences between SG-VIC and No Guidance. Similar to [104], our approach could decrease the completion time of a robot teleoperation task using variable guidance forces. However, they have not used learning-based method for generating guidance forces and also they have not used statistical analysis to support the effectiveness of their method compared to no guidance mode. Furthermore, using learning-based guidance/reproduction, similar results (the reduction of task completion time) have been reported in haptic teleoperation HRI [95], learning-based haptic guidance [4, 23], and LfD-based approaches [8, 68].
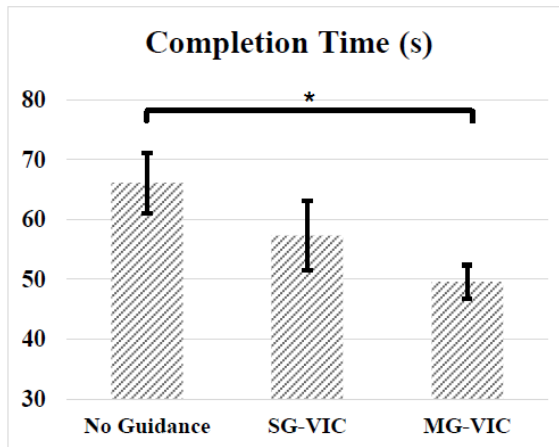
Figure 21: The graph represents the time of task completion in seconds for various methods involving steering wheel and gas pedal. This figure also shows that the MG-VIC approach is significantly more effective compared to the no guidance method. * marks significant differences with $P < 0.05$.
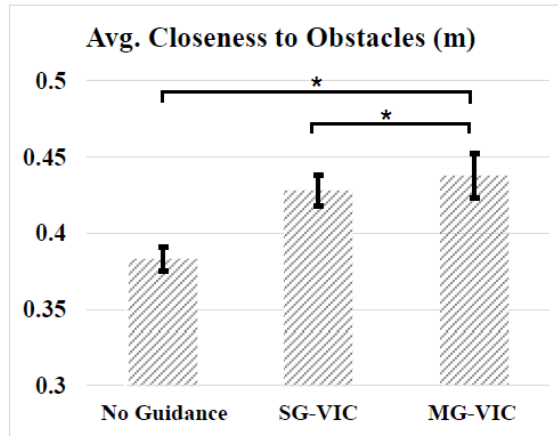
Figure 22: This graph represents the average closeness to the obstacles. As well as the other performance measurements, the MG-VIC method has provided better assistance to the participants. $*$ shows significant differences with $P < 0.05$.

Fig. 22 represents the average closeness of the robot to the obstacles, indicating how far the robot is able to travel pass the subjects. The figure demonstrates a trend among the different methods in terms of the average closeness to the obstacles. When no guidance is provided, the participants were moving at their discretion. For the other methods, when the MG-VIC method was used for applying guidance, the participants were able to pass the obstacles significantly further, compared to No Guidance.

Overall, it can be concluded that the MG-VIC method for providing LbG force has increased the performance of the users in maneuvering a teleoperated robot. Although, MG-VIC are not significantly better than SG-VIC for all three performance metrics, completion time for MG-VIC are significantly better than for No Guidance, while there is not significant difference between G-VIC and No Guidance. Furthermore, the results confirm that providing guidance force (MG-VIC and SG-VIC modes)

97

in general could be an effective way for assisting the users in terms of obstacle avoidance, increasing the speed of performing the task, and average closeness to obstacles.

An advantage of the LbG approach, which is an LfD-based approach, over *non-learning-based* guidance methods [16,19,29,31] is the generalization of demonstrated motions onto similar motion in novel situations. The LbG can generalize the motions in case of novel start pose without requiring intervention or further adaptation. To provide guidance for every novel task, adaption procedures (i.e. the trial and error method) should be used to tune the constant/adaptive gains. However, the available LbG skill models can be readily used to provide guidance forces for the novel tasks.

Table 7: One-Way ANOVA table for the performance metrics. NC: No. of Collisions, TC: Time of Completion, AC: Average Closeness, NG: No Guidance, SG: Single-Gain Variable Impedance Control, MG: Multiple-Gain Variable Impedance Control.

Metric	*Mean±SE NG*	*Mean±SE SG*	*Mean±SE MG*	*F (2,19)*	*P-Value*
NC (%)	55.50±3.24	41.00±2.39	34.00±1.97	17.91	< 0.001
TC (s)	66.09±5.06	57.29±5.83	49.56±2.84	3.02	0.04
AC (m)	0.43±0.014	0.42±0.010	0.38±0.007	6.67	0.002

4.4   Conclusions

In this chapter, a learning-based guidance (LbG) approach was introduced for providing assistance to the teleoperation of teleoperated robots by learning from expert

demonstrations. Using HMM, several skill models were developed from both kines-thetic and teleoperation demonstrations to adjust adaptive impedance control gains for generating guidance forces on steering and gas pedal. The skill models and a modified GMR were also incorporated into the LbG approach to produce continuous steering and pedal trajectories. The approach aim to not only encourage users to perform navigating tasks similar to experts, in terms of the desired position and ve-locity of steering and pedal, but also avoid them to collide obstacles. To achieve this goal, the impedance control gains were adapted based on learning-based stiffness and damping gains as well as the relative position and velocity of the teleoperated robot to obstacles.

To evaluate the proposed approach, single-gain variable impedance control (SG-VIC) and multiple-gain variable impedance control (MG-VIC) methods were devel-oped for generating LbG forces and their effectiveness on improving the performance of users were compared to no guidance. The performance metrics included number of collisions with the obstacles in the task, time of completing a considered task, and how close to the obstacles could the robot maneuver. The results confirmed that using different skill model, providing learning-based guidance forces were an effective way of assisting teleoperator maneuverings in terms of user performance. Furthermore, among the considered strategies for providing LbG forces, the MG-VIC method had a lead in improving the performance of the participants, by the incorporation of the velocity of the steering, pedal, the robot movements into both skill models and the variable impedance control strategies.

As future work, a library of skill models can be developed regarding the primitive motions of steering/pedal or teleoperators. The motions will be segmented using skill models and resulting LbG forces will be provided based on each corresponding primitive model. This segmentation would facilitate the generalization of tasks in case of novel combination of the primitive motions without requiring further adaptation. By training a library of primitive motions from demonstrations, various combination of motions would be considered as novel tasks.

Chapter 5

Conclusion and Future Work

The main objective of this thesis was to develop learning-based approaches for transferring skill from experts (teachers) to novices (learners) in physical human robot interaction. To achieve this goal, statistical models (machine learning techniques) were used to learn primitive motions from the expert demonstrations. The motion of human/robot were segmented into atomic and simple movements, primitive motions, to enable the approaches to provide more precise guidance forces. This also facilitates the generalization of the approaches to various dynamic tasks that include recognizable primitive motions. In this thesis, surgical gesture, motion of surgical drill within bone layers, and teleoperator maneuvers were considered as primitive motions. In reproduction phase, by using the learned models, robots assisted novices to perform dynamic tasks similar to the experts.

5.1 Conclusions

In the first main part of this thesis, an adaptive haptic guidance (HG) approach, as an LbG approach, was proposed based on the statistical models of gestures for HRI. A virtual surgical training task was segmented into gestures for modeling purposes and providing guidance forces to users via a robot manipulator. Due to the human stochastic behavior and the sequential nature of the tasks, statistical models (HMMs and HCRF) were developed to generate variable controlled forces according to the gestural differences. The stiffness gains were adjusted in real time regarding the gesture similarity between the user gesture and the models. The gesture-based variable impedance approach was enabled users to complete a task with better performance while balancing between completion time, motion smoothness, and average angular error, compared with no HG and constant HG conditions.

The utilization of discriminative approach compared to generative approach for providing adaptive HG was promising to improve user performance for completing dynamic tasks. There was no linear mapping between the recognition accuracy of the statistical gesture models and the performance outcomes of the HG approaches. Moreover, only statistical modeling methods with a low computationally complexity are well-suited for real-time haptic rendering. HMM and HCRF were successfully applicable to generating real-time guidance forces, which can significantly increase the pace of motor-learning in training systems.

To train statistical models, features can be selected regarding the characteristics

of the primitive motions. For instance, if the primitive motions are end-effector movements in orthogonal direction, the linear position, velocity and acceleration of the tool tip would be chosen as features. To train more complex tasks/motions, including positioning needle, making C loop, and pulling suture, other kinematic/kinesthetic variables, including the rotational velocity and rotation matrix of the tool tip, end-effector force as well as video data, may be added to the features. This facilitates the recognition of complexed primitive motions and consequently the production of effective LbG forces.

In the second part of the thesis, to further show the effectiveness of the guidance approach, it was adapted for a kinesthetic HRI simulation that aims to transfer the skills of expert surgeons to resident trainees. During the learning phase, the expert demonstrations were used to develop an expert HCRF model for learning the stiffness variations of different bone layers. To discriminate the skill levels of an unknown-skill user, a novice HCRF model was also developed from the demonstration of novice residents. As a result, the skill levels of a user was determined by comparing user observations with the both HCRF skill models. In practice phase, using stiffness variations captured by the expert HCRF, the LbG approach was able to guide the trainees for performing training tasks similar to the experts.

The approach was used for both skill discrimination and user performance improvement in a virtual reality-based (VR-based) simulation of femur drilling surgery. Real CT data were used to provide the users with the feeling of bone stiffness variations in regard to the drilled depth. HCRF-based skill models (expert HCRF and

resident HCRF) were developed to segment the drill motion within different bone layers, differentiate user's skill as experts or residents, and assist residents with applying appropriate drilling forces within different bone layers. A set of performance metrics, including task completion time, RMSE for position, and average bone temperature, was also used to objectively evaluate the skills of users.

The results of a clinical study confirmed that providing residents with the LbG approach resulted in significant performance improvements in terms of drilling task completion time and average femur temperature. However, the improvements could not enable the residents to perform the femur drilling in a similar skill level of the experts. In addition, the results showed that not only the skill models, but also performance metrics could be used for discriminating the skill level of users.

In the final part of the thesis, in order to teleoperate a robot, a modified learning-based guidance approach was used to assist operators in HRI. A set of expert operator demonstrations were used to develop driving skill model. The temporal and spatial variation of demonstrations were encoded using hidden Markov model (HMM) as the skill model. A modified GMR in combination with the HMM is also developed to produce a state of reference motion. Applied forces were adaptively computed in real time regarding the similarities between the maneuver of users and the skill model. The learning-based guidance aimed to encourage users to navigate the robot similar to the expert operators. Using an experimental setup, the teleoperated robot was navigated through a haptic steering wheel and a haptic gas pedal. The performance of the users was improved when LbG guidance forces were assisting the users to

perform a robot teleoperation task.

5.2   Future Work

Overall, discriminative-based approaches, in comparison with generative-based approaches, provide more effective adaptive guidance forces in terms of user performance. However, to take advantages of both models, a combination of generative and discriminative LbG approaches can be developed using learning from demonstration (LfD). Generative-based skill models would enable generation of continuous reference trajectory from expert demonstrations in the learning phase, while using discriminative-based skill models will generate more effective LbG forces in reproduction/practice phase.

The proposed LbG approaches can be investigated by expanding the skill models with more gestures/motions/maneuvers. Considering more gestures, the approaches can be investigated in more complex and realistic tasks. Furthermore, extensive human factor studies can be conducted to analyze the effect of task complexity on the efficacy of the approaches and discover the parameters that may affect the outcomes of such LbG-enabled systems in pHRI.

The learning effect of the proposed LbG approach can be studied. The focus of this work was on providing assistance to users for improving their *performance*. However, the effect of the LbG approaches on *learning* particular skills can be examined by designing appropriate user studies. A potential experimental study would

be as follows. This study will employ a quasi-experimental pre/posttest design. At pretest, both groups will perform a training task without guidance. Participants will be randomly assigned to either Group one or Group two. The participants of Group one will perform the task with LbG 15 times, while Group two will only perform the same trials without guidance. After posttest, Group one will do a new task without guidance while Group two will be providing by LbG. Finally, a delayed posttest will be conducted to investigate the effect of skill learning. This design will be able to reveal that participants will learn any new motor skill or would be getting more and more specialized in performing a specific task by carrying out the task several trials. Finally, it will be investigated how well the LbG steepen the learning curve.

In addition to end-effector kinematics, the kinematics of upper limb movements can be incorporated into statistical skill models for developing more effective LbG approaches. We developed a VR-based simulation that incorporated upper limbs movements into measuring user performance and the discrimination of skill levels. The early results indicated that the motion of upper limb joints can be used to discriminate an expert user from a novice user [109]. The results also showed that the dominant hand performance decreased while non-dominant hand was engaged on a task. As a future work, the kinematics of the end-effector and both upper limbs will be utilized to develop the skill models and generate LbG through the end-effector and wearable vibrotactile actuators for encouraging users to perform correct hand gestures.

Considering the rapid advancement of computing technology in recent years, the

large collection of features can be processed in real time. This provide an opportunity to fuse vision and kinesthetic data from many cameras/sensors into the learning-based approach for improving the recognition accuracy and generating more precise guidance forces. In addition, the use of larger datasets could possibly improve a) the training of large skill models in terms of capturing hidden skills and b) the fine-tuning of the parameters of LbG approaches.

By collecting or accessing large datasets of the primitive motions, deep learning based guidance (D-LbG) approaches can be developed to better guide, classify, and segment a user motions in pHRI. Big data analytics and deep learning are two active research fields in data science and machine learning. While data keep getting bigger, deep learning may be used to take advantage of the predictive power of big data [110]. A significant importance of using deep learning is to analyze and learn massive amounts of unlabeled data since raw data are largely unlabeled [111]. Deep learning has widely been utilized in several big data domains, including computer vision [112] and speech recognition [113], to improve classification results. As a result, using deep learning and big data algorithms are promising for developing deep skill models and the provision of D-LbG forces as well as the segmentation and recognition of the user motions.

In addition, the outcomes of this thesis can be used in other fields such as rehabilitation, sport training, autonomous driving, and mobile robot navigation. The skill of healthy people, sport coaches, or drivers can be transfered to designated robotic

systems that will be able to assist humans for performing dynamic tasks (in rehabilitation or sport training) or autonomously carry out tasks (in driving or mobile robot navigation).

Bibliography

[1] W. Yu, O. Chuy Jr, E. G. Collins Jr, and P. Hollis, "Dynamic modeling of a skid-steered wheeled vehicle with experimental verification," *International Conference on Intelligent Robots and Systems, IROS*, pp. 4212–4219, 2009.

[2] M. A. Goodrich and A. C. Schultz, "Human-robot interaction: a survey," *Foundations and trends in human-computer interaction*, vol. 1, no. 3, pp. 203–275, 2007.

[3] B. D. Argall, S. Chernova, M. Veloso, and B. Browning, "A survey of robot learning from demonstration," *Robotics and autonomous systems*, vol. 57, no. 5, pp. 469–483, 2009.

[4] E. Zahedi, J. Dargahi, M. Kia, and M. Zadeh, "Gesture-based adaptive haptic guidance: A comparison of discriminative and generative modeling approaches," *IEEE Robotics and Automation Letters*, vol. 2, no. 2, pp. 1015–1022, 2017.

[5] A. Billard, S. Calinon, R. Dillmann, and S. Schaal, "Robot programming by demonstration, chapter 59," in *Springer handbook of robotics*, pp. 1371–1394, Springer, 2008.

[6] L. Rozo, P. Jiménez, and C. Torras, "A robot learning from demonstration framework to perform force-based manipulation tasks," *Intelligent service robotics*, vol. 6, no. 1, pp. 33–51, 2013.

[7] L. Rozo, S. Calinon, D. G. Caldwell, P. Jimenez, and C. Torras, "Learning physical collaborative robot behaviors from human demonstrations," *IEEE Transactions on Robotics*, vol. 32, no. 3, pp. 513–527, 2016.

[8] K. Kronander and A. Billard, "Learning compliant manipulation through kinesthetic and tactile human-robot interaction," *IEEE Transactions on Haptics*, vol. 7, no. 3, pp. 367–380, 2014.

[9] A. Bernardino, M. Henriques, N. Hendrich, and J. Zhang, "Precision grasp synergies for dexterous robotic hands," in *Robotics and Biomimetics (ROBIO), 2013 IEEE International Conference on*, pp. 62–67, 2013.

[10] S. Calinon and A. Billard, "Incremental learning of gestures by imitation in a humanoid robot," in *Proceedings of the ACM/IEEE international conference on Human-robot interaction*, pp. 255–262, 2007.

[11] E. Cha, K. Kronander, and A. Billard, "Combined kinesthetic and simulated interface for teaching robot motion models," in *Robot and Human Interactive Communication (RO-MAN), 2015 24th IEEE International Symposium on*, pp. 83–88, IEEE, 2015.

[12] J. Aleotti, S. Caselli, and M. Reggiani, "Leveraging on a virtual environment for robot programming by demonstration," *Robotics and Autonomous Systems*, vol. 47, no. 2, pp. 153–161, 2004.

[13] J. Aleotti, S. Caselli, and M. Reggiani, "Evaluation of virtual fixtures for a robot programming by demonstration interface," *IEEE Transactions on Systems, Man, and Cybernetics-Part A: Systems and Humans*, vol. 35, no. 4, pp. 536–545, 2005.

[14] S. Bowyer, B. L. Davies, F. Baena, and Y. Rodriguez, "Active constraints/virtual fixtures: A survey," *IEEE Transactions on Robotics*, vol. 30, no. 1, pp. 138–157, 2013.

[15] J. Bluteau, S. Coquillart, Y. Payan, and E. Gentaz, "Haptic guidance improves the visuo-manual tracking of trajectories," *PloS one*, vol. 3, p. e1775, jan 2008.

[16] D. Powell and M. K. O'Malley, "The task-dependent efficacy of shared-control haptic guidance paradigms," *IEEE Transactions on Haptics*, vol. 5, no. 3, pp. 208–219, 2012.

[17] A. Bettini, S. Lang, A. Okamura, and G. Hager, "Vision assisted control for manipulation using virtual fixtures," *IEEE Transactions on Robotics*, vol. 2, pp. 1171–1176, 2004.

[18] W. Yu, R. Alqasemi, and R. Dubey, "Telemanipulation Assistance Based on Motion Intention Recognition," *IEEE International Conference on Robotics and Automation (ICRA)*, pp. 21–26, April 2005.

[19] A. Safavi, L. Huynh, H. Rahmat-Khah, E. Zahedi, and M. H. Zadeh, "A novel mpc approach to optimize force feedback for human-robot shared control," *2015 IEEE/RSJ International Conference on Intelligent Robots and Systems (IROS 2015)*, pp. 3018–3023, Sept. 28-Oct. 2 2015.

[20] A. Safavi and M. Zadeh, "Model-based haptic guidance in surgical skill improvement," *2015 IEEE International Conference on Systems, Man, and Cybernetics (SMC 2015)*, pp. 1104–1109, 9-12 Oct. 2015.

[21] A. De Santis, B. Siciliano, A. De Luca, and A. Bicchi, "An atlas of physical human-robot interaction," *Mechanism and Machine Theory*, vol. 43, no. 3, pp. 253–270, 2008.

[22] J. Medina, D. Lee, and S. Hirche, "Risk-Sensitive Optimal Feedback Control for Haptic Assistance," *IEEE International Conference on Robotics and Automation (ICRA)*, pp. 1025–1031, May 2012.

[23] J. Medina, T. Lorenz, and S. Hirche, "Synthesizing Anticipatory Haptic Assistance Considering Human Behavior Uncertainty," *IEEE Transactions on Robotics*, vol. 31, no. 1, pp. 180–190, 2015.

[24] C. Reiley and G. Hager, "Task versus subtask surgical skill evaluation of robotic minimally invasive surgery," *Medical Image Computing and Computer-Assisted Intervention (MICCAI)*, pp. 435–442, 2009.

[25] S. Schaal, A. Ijspeert, and A. Billard, "Computational approaches to motor learning by imitation," *Philosophical Transactions of the Royal Society B: Biological*, no. February, pp. 537–547, 2003.

[26] A. Y. Ng and M. I. Jordan, "On discriminative vs. generative classifiers: A comparison of logistic regression and naive bayes," *Advances in neural information processing systems*, pp. 841–848, 2002.

[27] L. Tao, L. Zappella, G. D. Hager, and R. Vidal, "Surgical gesture segmentation and recognition," *Medical Image Computing and Computer-Assisted Intervention MICCAIs*, pp. 339–346, 2013.

[28] N. Hogan, "Impedance control: An approach to manipulation: I - theory. ii - implementation. iii - applications," *Journal of Dynamic Systems, Measurement, and Control*, vol. 107, no. 1, pp. 8–16, 1985.

[29] M. Li and A. Okamura, "Recognition of Operator Motions for Real-Time Assistance using Virtual Fixtures," *Haptic Interfaces for Virtual Environment and Teleoperator Systems (HAPTICS)*, pp. 22–23, March 2003.

[30] M. Power, H. Rafii-tari, C. Bergeles, V. Vitiello, and G. Yang, "A Cooperative Control Framework For Haptic Guidance Of Bimanual Surgical Tasks Based On

Learning From Demonstration," *IEEE International Conference on Robotics and Automation (ICRA)*, pp. 5330–5337, 2015.

[31] C. Passenberg, A. Glaser, and A. Peer, "Exploring the design space of haptic assistants: The assistance policy module," *IEEE Transactions on Haptics*, vol. 6, no. 4, pp. 440–452, 2013.

[32] D. Kulic, D. Kragic, and V. Krüger, "Learning action primitives," *Visual analysis of humans*, pp. 333–353, 2011.

[33] C. M. Bishop and J. Lasserre, "Generative or discriminative? getting the best of both worlds," *Bayesian statistics*, vol. 8, pp. 3–24, 2007.

[34] Ghasemzadeh H., Loseu V. and Jafari R., "Wearable coach for sport training: A quantitative model to evaluate wrist-rotation in golf," *Journal of Ambient Intelligence and Smart Environments*, vol. 1, no. 2, pp. 173–184, 2009.

[35] MilesH.C., Pop S.R., Watt S.J., Lawrence G.P. and John N.W., "A review of virtual environments for training in ball sports," *Computers & Graphics*, vol. 36, no. 6, pp. 714–726, 2012.

[36] Zhou H. and Hu H., "Human motion tracking for rehabilitation – A survey," *Biomedical Signal Processing and Control*, vol. 3, no. 1, pp. 1–18, 2008.

[37] O. Khatib, K. Yokoi, O. Brock, K. Chang, and A. Casal, "Robots in Human Environments : Basic Autonomous Capabilities," *The International Journal of Robotics Research*, vol. 18, no. 7, pp. 684–696, 1999.

[38] S. Thrun, "Probabilistic algorithms in robotics," *Ai Magazine*, vol. 21, no. 4, p. 93, 2000.

[39] D. Lee and C. Ott, "Incremental kinesthetic teaching of motion primitives using the motion refinement tube," *Autonomous Robots*, vol. 31, no. 2-3, pp. 115–131, 2011.

[40] K. Kahol, N. Krishnan, V. Balasubramanian, S. Panchanathan, M. Smith, and J. Ferrara, "Measuring movement expertise in surgical tasks," pp. 719–722, 2006.

[41] S. Wang, A. Quattoni, L. Morency, D. Demirdjian, and T. Darrell, "Hidden conditional random fields for gesture recognition," *Computer Vision and Pattern Recognition, 2006 IEEE Computer Society Conference on*, vol. 2, pp. 1521–1527, 2006.

[42] W. Lu, Z. Tong, and J. Chu, "Dynamic hand gesture recognition with leap motion controller," *IEEE Signal Processing Letters*, vol. 23, no. 9, pp. 1188–1192, 2016.

[43] W.-T. Hong, "Hcrf-based model compensation for noisy speech recognition," pp. 277–278, 2013.

[44] D. Feygin, M. Keehner, and R. Tendick, "Haptic guidance: experimental evaluation of a haptic training method for a perceptual motor skill," *Proceedings*

10th Symposium on Haptic Interfaces for Virtual Environment and Teleoperator Systems, pp. 40–47, 2002.

[45] J. Liu, S. C. Cramer, and D. J. Reinkensmeyer, "Learning to perform a new movement with robotic assistance: comparison of haptic guidance and visual demonstration.," *Journal of neuroengineering and rehabilitation*, vol. 3, p. 20, 2006.

[46] Y. Blandin, L. Lhuisset, and L. Proteau, "Cognitive Processes Underlying Observational Learning of Motor Skills," *Quarterly Journal of Experimental Psychology Section A Human Experimental Psychology*, vol. 52A, no. 4, pp. 957–979, 1999.

[47] G. Megali, S. Sinigaglia, O. Tonet, and P. Dario, "Modelling and evaluation of surgical performance using hidden Markov models," *IEEE Transactions on Biomedical Engineering*, vol. 53, no. 10, pp. 1911–1919, 2006.

[48] L. Yang, Y. Xu, and C. Chen, "Human action learning via hidden Markov model," *IEEE Transactions on Systems, Man and Cybernetics, Part A: Systems and Humans*, vol. 27, no. 1, pp. 34–44, 1997.

[49] J. Rosen, J. Brown, L. Chang, M. Sinanan, and B. Hannaford, "Generalized approach for modeling minimally invasive surgery as a stochastic process using a discrete Markov model," *IEEE Transactions on Biomedical Engineering*, vol. 53, no. 3, pp. 399–413, 2006.

[50] K. P. Murphy, *Machine learning: a probabilistic perspective.* MIT press, 2012.

[51] K. Kahol, M. Vankipuram, and M. Smith, "Cognitive simulators for medical education and training," *Journal of Biomedical Informatics*, vol. 42, no. 4, pp. 593–604, 2009.

[52] S. Cotin, N. Stylopoulos, M. Ottensmeyer, P. Neumann, D. Rattner, and S. Dawson, "Metrics for Laparoscopic Skills Trainers: The Weakest Link!," *Medical Image Computing and Computer-Assisted Intervention (MICCAI)*, pp. 35–43, 2002.

[53] L. Rabiner, "A tutorial on hidden Markov models and selected applications in speech recognition," *Proceedings of the IEEE*, vol. 77, no. 2, pp. 257–286, 1989.

[54] J. Nocedal and S. Wright, *Numerical optimization.* Springer Science & Business Media, 2006.

[55] M. Smid, "Handbook of computational geometry," 2000.

[56] N. Diolaiti, G. Niemeyer, F. Barbagli, and J. K. Salisbury, "Stability of haptic rendering: Discretization, quantization, time delay, and coulomb effects," *IEEE Transactions on Robotics*, vol. 22, no. 2, pp. 256–268, 2006.

[57] R. J. Adams and B. Hannaford, "Stable haptic interaction with virtual environments," *IEEE Transactions on robotics and Automation*, vol. 15, no. 3, pp. 465–474, 1999.

[58] C. Lea, G.D. Hager, and R. Vidal, "An improved model for segmentation and recognition of fine-grained activities with application to surgical training tasks," *IEEE Winter Conference on In Applications of Computer Vision (WACV)*, pp. 1123–1129, 2015.

[59] D. Schapira and C. Schapira, "Osteoporosis: the evolution of a scientific term," *Osteoporosis International*, vol. 2, no. 4, pp. 164–167, 1992.

[60] S. Wade, C. Strader, L. Fitzpatrick, M. Anthony, and C. O'Malley, "Estimating prevalence of osteoporosis: examples from industrialized countries," *Archives of osteoporosis*, vol. 9, no. 1, p. 182, 2014.

[61] M. J. Goldacre, S. E. Roberts, and D. Yeates, "Mortality after admission to hospital with fractured neck of femur: database study," *Bmj*, vol. 325, no. 7369, pp. 868–869, 2002.

[62] K.-G. Thorngren, "National registration of hip fractures," 2008.

[63] T. Coles, D. Meglan, and N. John, "The Role of Haptics in Medical Training Simulators : A Survey of the State of the Art," *IEEE Transactions on Haptics*, vol. 4, no. 1, pp. 51–66, 2011.

[64] G. Ahlberg, *The role of simulation technology for skills acquisition in image guided surgery.* Institutionen för kirurgisk vetenskap/Department of Surgical Science, 2005.

[65] N. Seymour, "VR to OR: a review of the evidence that virtual reality simulation improves operating room performance," *World journal of surgery*, vol. 32, pp. 182–8, feb 2008.

[66] W. Chi, H. Rafii-Tari, C. J. Payne, J. Liu, C. Riga, C. Bicknell, and G.-Z. Yang, "A learning based training and skill assessment platform with haptic guidance for endovascular catheterization," in *IEEE International Conference on Robotics and Automation (ICRA)*, pp. 2357–2363, IEEE, 2017.

[67] V. Koropouli, D. Lee, and S. Hirche, "Learning interaction control policies by demonstration," in *Intelligent Robots and Systems (IROS), 2011 IEEE/RSJ International Conference on*, pp. 344–349, IEEE, 2011.

[68] P. Kormushev, S. Calinon, and D. G. Caldwell, "Imitation learning of positional and force skills demonstrated via kinesthetic teaching and haptic input," *Advanced Robotics*, vol. 25, no. 5, pp. 581–603, 2011.

[69] J. C. Teo, K. M. Si-Hoe, J. E. Keh, and S. H. Teoh, "Relationship between ct intensity, micro-architecture and mechanical properties of porcine vertebral cancellous bone," *Clinical biomechanics*, vol. 21, no. 3, pp. 235–244, 2006.

[70] R. E. Sofronia, A. Davidescu, and G. G. Savii, "Towards a virtual reality simulator for orthognathic basic skils," in *Applied Mechanics and Materials*, vol. 162, pp. 352–357, 2012.

[71] T. N. Bogoni and M. S. Pinho, "Haptic technique for simulating multiple density materials and material removal," 2013.

[72] Y. Liu and S. D. Laycock, "A haptic system for drilling into volume data with polygonal tools.," in *TPCG*, pp. 9–16, 2009.

[73] D. Morris, C. Sewell, N. Blevins, F. Barbagli, and K. Salisbury, "A collaborative virtual environment for the simulation of temporal bone surgery," in *International Conference on Medical Image Computing and Computer-Assisted Intervention*, pp. 319–327, 2004.

[74] M. E. Müller, M. Allgöwer, and S. Perren, *Manual of internal fixation: techniques recommended by the AO-ASIF group*. Springer Science & Business Media, 1991.

[75] T. D. Brown and A. B. Ferguson, "Mechanical property distributions in the cancellous bone of the human proximal femur," *Acta Orthopaedica Scandinavica*, vol. 51, no. 1-6, pp. 429–437, 1980.

[76] R. K. Pandey and S. Panda, "Drilling of bone: A comprehensive review," *Journal of clinical orthopaedics and trauma*, vol. 4, no. 1, pp. 15–30, 2013.

[77] V. Boner, P. Kuhn, T. Mendel, and A. Gisep, "Temperature evaluation during pmma screw augmentation in osteoporotic bone- an in vitro study about the risk of thermal necrosis in human femoral heads," *Journal of Biomedical Materials Research Part B: Applied Biomaterials*, vol. 90, no. 2, pp. 842–848, 2009.

[78] A. Pourkand, C. Salas, J. Regalado, K. Bhakta, R. Tufaro, D. Mercer, and D. Grow, "Objective evaluation of motor skills for orthopedic residents using a motion tracking drill system: Outcomes of an abos approved surgical skills training program," *The Iowa orthopaedic journal*, vol. 36, p. 13, 2016.

[79] J. Pettersson, K. L. Palmerius, H. Knutsson, O. Wahlstrom, B. Tillander, and M. Borga, "Simulation of patient specific cervical hip fracture surgery with a volume haptic interface," *IEEE transactions on biomedical engineering*, vol. 55, no. 4, pp. 1255–1265, 2008.

[80] C. E. Reiley, E. Plaku, and G. D. Hager, "Motion Generation of Robotic Surgical Tasks : Learning From Expert Demonstrations," *Engineering in Medicine and Biology Society*, pp. 967–970, 2010.

[81] M. K. Chmarra, S. Klein, J. C. de Winter, F.-W. Jansen, and J. Dankelman, "Objective classification of residents based on their psychomotor laparoscopic skills," *Surgical endoscopy*, vol. 24, no. 5, pp. 1031–1039, 2010.

[82] T. B. Sheridan, "Human-robot interaction: status and challenges," *Human factors*, vol. 58, no. 4, pp. 525–532, 2016.

[83] S. M. Erlien, S. Fujita, and J. C. Gerdes, "Shared steering control using safe envelopes for obstacle avoidance and vehicle stability," *IEEE Transactions on Intelligent Transportation Systems*, vol. 17, no. 2, pp. 441–451, 2016.

[84] D. A. Abbink, M. Mulder, and E. R. Boer, "Haptic shared control: smoothly shifting control authority?," *Cognition, Technology & Work*, vol. 14, no. 1, pp. 19–28, 2012.

[85] P. Boehm, A. H. Ghasemi, S. O'Modhrain, P. Jayakumar, and R. B. Gillespie, "Architectures for shared control of vehicle steering," *IFAC-PapersOnLine*, vol. 49, no. 19, pp. 639–644, 2016.

[86] P. Pastor, H. Hoffmann, T. Asfour, and S. Schaal, "Learning and generalization of motor skills by learning from demonstration," in *Robotics and Automation, 2009. ICRA'09. IEEE International Conference on*, pp. 763–768, IEEE, 2009.

[87] L. Peternel and J. Babič, "Learning of compliant human–robot interaction using full-body haptic interface," *Advanced Robotics*, vol. 27, no. 13, pp. 1003–1012, 2013.

[88] P. Abbeel, A. Coates, M. Quigley, and A. Y. Ng, "An application of reinforcement learning to aerobatic helicopter flight," in *Advances in neural information processing systems*, pp. 1–8, 2007.

[89] P. Abbeel, D. Dolgov, A. Y. Ng, and S. Thrun, "Apprenticeship learning for motion planning with application to parking lot navigation," in *Intelligent Robots and Systems, 2008. IROS 2008. IEEE/RSJ International Conference on*, pp. 1083–1090, IEEE, 2008.

[90] K. Kukliński, K. Fischer, I. Marhenke, F. Kirstein, V. Maria, N. Krüger, T. R. Savarimuthu, *et al.*, "Teleoperation for learning by demonstration: Data glove versus object manipulation for intuitive robot control," in *Ultra Modern Telecommunications and Control Systems and Workshops (ICUMT), 2014 6th International Congress on*, pp. 346–351, IEEE, 2014.

[91] A. Murali, S. Sen, B. Kehoe, A. Garg, S. McFarland, S. Patil, W. D. Boyd, S. Lim, P. Abbeel, and K. Goldberg, "Learning by observation for surgical subtasks: Multilateral cutting of 3d viscoelastic and 2d orthotropic tissue phantoms," in *Robotics and Automation (ICRA), 2015 IEEE International Conference on*, pp. 1202–1209, IEEE, 2015.

[92] M. Mulder, D. Abbink, M. M. Van Paassen, M. Mulder, *et al.*, "Design of a haptic gas pedal for active car-following support," *IEEE Transactions on Intelligent Transportation Systems,*, vol. 12, no. 1, pp. 268–279, 2011.

[93] L. Rozo, S. Calinon, D. G. Caldwell, P. Jimenez, and C. Torras, "Learning physical collaborative robot behaviors from human demonstrations," *IEEE Transactions on Robotics*, vol. 32, no. 3, pp. 513–527, 2016.

[94] S. Calinon, F. D'halluin, D. G. Caldwell, and A. G. Billard, "Handling of multiple constraints and motion alternatives in a robot programming by demonstration framework," in *Humanoid Robots, 2009. Humanoids 2009. 9th IEEE-RAS International Conference on*, pp. 582–588, IEEE, 2009.

[95] J. R. Medina, M. Lawitzky, A. Mörtl, D. Lee, and S. Hirche, "An experience-driven robotic assistant acquiring human knowledge to improve haptic cooperation," in *Intelligent Robots and Systems (IROS), 2011 IEEE/RSJ International Conference on*, pp. 2416–2422, IEEE, 2011.

[96] E. Garcia, M. A. Jimenez, P. G. De Santos, and M. Armada, "The evolution of robotics research," *IEEE Robotics and Automation Magazine*, vol. 14, pp. 90–103, 2007.

[97] D. Kulić, W. Takano, and Y. Nakamura, "Incremental learning, clustering and hierarchy formation of whole body motion patterns using adaptive hidden markov chains," *The International Journal of Robotics Research*, vol. 27, no. 7, pp. 761–784, 2008.

[98] S. Calinon, F. D'halluin, E. L. Sauser, D. G. Caldwell, and A. G. Billard, "Learning and reproduction of gestures by imitation," *IEEE Robotics and Automation Magazine*, vol. 17, no. 2, pp. 44–54, 2010.

[99] Z. Yang, K. Ito, K. Saijo, K. Hirotsune, A. Gofuku, and F. Matsuno, "A combined navigation strategy by a steering wheel and a mouse for a tank rescue robot," *International Conference on Robotics and Biomimetics, ROBIO*, pp. 239–244, 2004.

[100] N. Diolaiti and C. Melchiorri, "Teleoperation of a mobile robot through haptic feedback," *International Workshop on Haptic Virtual Environments and Their Applications, HAVE*, pp. 67–72, 2002.

[101] I. Elhajj, N. Xi, W. K. Fung, Y. H. Liu, W. J. Li, T. Kaga, and T. Fukuda, "Haptic information in internet-based teleoperation," *IEEE/ASME Transactions on Mechatronics*, vol. 6, no. 3, pp. 295–304, 2001.

[102] T. Fong, C. Thorpe, and C. Baur, "Advanced interfaces for vehicle teleoperation: Collaborative control, sensor fusion displays, and remote driving tools," *Autonomous Robots*, vol. 11, no. 1, pp. 77–85, 2001.

[103] P. Richard and P. Coiffet, "Human perceptual issues in virtual environments: sensory substitution and information redundancy," *4th International Workshop on Robot and Human Communication, RO-MAN*, pp. 301–306, 1995.

[104] I. Farkhatdinov, J.-H. Ryu, and J. An, "A preliminary experimental study on haptic teleoperation of mobile robot with variable force feedback gain," *IEEE Haptics Symposium*, pp. 251–256, 2010.

[105] A. H. Jamson, D. L. Hibberd, and N. Merat, "Interface design considerations for an in-vehicle eco-driving assistance system," *Transportation Research Part C: Emerging Technologies*, vol. 58, pp. 642–656, 2015.

[106] S. M. Petermeijer, D. A. Abbink, M. Mulder, and J. C. de Winter, "The effect of haptic support systems on driver performance: A literature survey," *IEEE transactions on haptics*, vol. 8, no. 4, pp. 467–479, 2015.

[107] T. Brandt, T. Sattel, and M. Bohm, "Combining haptic human-machine interaction with predictive path planning for lane-keeping and collision avoidance systems," in *IEEE Intelligent Vehicles Symposium*, pp. 582–587, 2007.

[108] S. M. Khansari-Zadeh and A. Billard, "Learning stable nonlinear dynamical systems with gaussian mixture models," *IEEE Transactions on Robotics*, vol. 27, no. 5, pp. 943–957, 2011.

[109] E. Zahedi, H. Rahmat-Khah, J. Dargahi, and M. Zadeh, "Virtual reality based training: Evaluation of user performance by capturing upper limb motion," in *2017 IEEE Virtual Reality (VR)*, pp. 255–256, 2017.

[110] X.-W. Chen and X. Lin, "Big data deep learning: challenges and perspectives," *IEEE access*, vol. 2, pp. 514–525, 2014.

[111] M. M. Najafabadi, F. Villanustre, T. M. Khoshgoftaar, N. Seliya, R. Wald, and E. Muharemagic, "Deep learning applications and challenges in big data analytics," *Journal of Big Data*, vol. 2, no. 1, p. 1, 2015.

[112] A. Krizhevsky, I. Sutskever, and G. E. Hinton, "Imagenet classification with deep convolutional neural networks," in *Advances in neural information processing systems*, pp. 1097–1105, 2012.

[113] G. Hinton, L. Deng, D. Yu, G. E. Dahl, A.-r. Mohamed, N. Jaitly, A. Senior, V. Vanhoucke, P. Nguyen, T. N. Sainath, *et al.*, "Deep neural networks for

acoustic modeling in speech recognition: The shared views of four research groups," *IEEE Signal Processing Magazine*, vol. 29, no. 6, pp. 82–97, 2012.